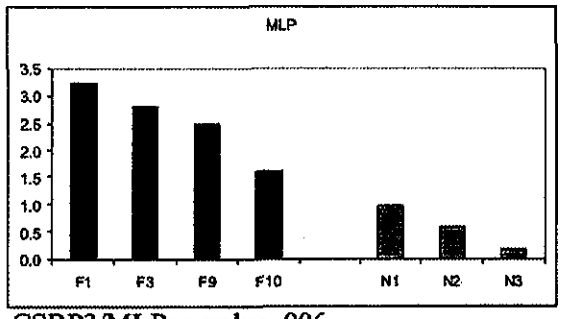

A CSRP3/MLP: p value .006

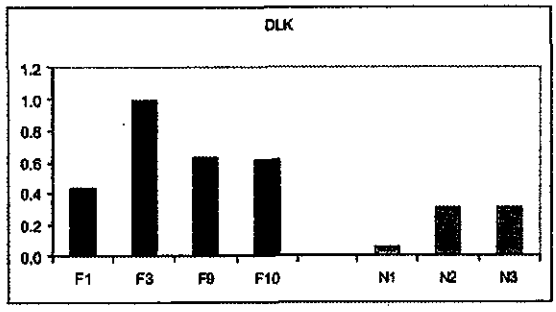

B DLK: p value .027

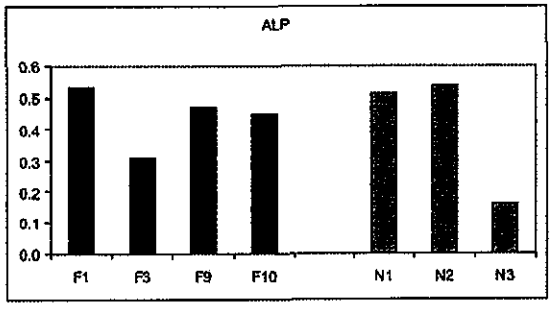

C ALP: p value .815

Figure 1. TaqMan (real-time PCR) analysis confirms the alteration of specific transcripts in FSHD muscle. PCR primers were generated for representative transcripts (MLP, DLK and ALP) expressed in muscle. Both MLP and DLK demonstrate increased expression in FSHD muscle (P-value <0.006 and <0.027, respectively), verifying corresponding GeneChip data. ALP is not altered in FSHD muscle, confirming the expression pattern on the U95A GeneChip.

DLK1 were significantly increased upon real-time RT-PCR analysis, while no difference in ALP levels was detected.

Expression changes in common with other muscular dystrophies

FSHD expression profiles were also compared to those generated for other muscular dystrophies using the identical GeneChip format (25). Several of the significantly dysregulated genes in FSHD muscle were also found to be affected in other types of muscular dystrophy (DMD, αSGD; Table 2). It is interesting to note that a large percentage of these genes is probably dysregulated as a result of fibrotic infiltration. These genes include such extracellular matrix proteins as collagen types I and VI, lumican, fibronectin and tenascin. Other categories of genes affected in common with other types of muscular dystrophy include immune response genes such as complement and coagulation factors, and genes involved in energy metabolism.

FSHD-specific genes that are involved in progression of the disease can be identified by comparing clinically affected versus unaffected muscles within single dystrophy patients

Matched pairs of muscle biopsies from affected and unaffected muscle within the same patient are an extremely valuable resource to monitor the progression of disease. Expression profiling of three sets of paired muscle samples (affected and unaffected muscle from each of three individuals) was performed on the HuFL GeneChip. Expression profiling of affected to unaffected muscle highlights the genes that correlate with progressive dystrophy. Table 3 lists the genes that are deregulated in affected FSHD muscle (greater than 50% of the 12 pairwise comparisons). Of the 12 genes, six (50%) represent a further dysregulation of genes involved in the dystrophic process, as these same genes are altered in other muscular dystrophies. The deregulation of these transcripts is likely to be a secondary effect that contributes to the symptoms or compensatory response in FSHD (as they correlate with progressive dystrophy), but not the early primary cause of the disease. The genes affecting cellular differentiation (CSRP3, TFRC, DLK1 and WEE1, listed in Table 1) are not further increased, and thus are likely to be related to the primary defect in FSHD. However, as FSHD affects specific muscle groups more severely than others, the possibility that primary changes are actually more pronounced in the affected muscle cannot be ruled out.

GeneChip expression analysis does not support a 4q35 position effect

Expression of 4q35 genes in FSHD muscle is summarized in Table 4. Eight FSHD region (4q35) genes are present on both the HuFL and U95A arrays, with an additional seven genes present on the U95A GeneChip. Using the same criteria (>2-fold change in expression, $P < 0.05$) we found that none of the genes in the 4q35 region are significantly altered. We find no elevation of FRG1 in this study, although are not able to discern 4q35-specific transcripts of this multi-copy gene as the hybridization-based approach used in this study allows only for the expression analysis of all FRG1-like sequences in the genome. However, for all single-copy genes in the 4q35 FSHD region (FACL2, ANT1, IRF2, KLKB1, FAT, CASP3, F11, TLR3, ALP, ING1L, ARGBP2, DCTD and DKF2P564J102), none exhibit a significantly altered pattern of expression in FSHD upon oligonucleotide microarray analysis.

Table 2. Common dysregulated genes in FSHD, DMD and α-SGD

Probe set	Gene description	*P*-value	Fold change FSHD	DMD	a-SGD
	Cell surface and extracellular matrix				
M55998	Alpha-1 collagen type I	1.91×10^{-5}	5	6	5
X15882	Collagen, type VI, alpha 2	4.50×10^{-3}	2	nc	6
Z74616	Collagen, type I, alpha 2	6.74×10^{-3}	5	6	5
32307	Collagen, type I, alpha 2	1.91×10^{-4}	3	6	5
X02761	Fibronectin 1	1.49×10^{-2}	3	4	3
31719	Fibronectin 1	9.16×10^{-4}	2	4	3
38038	Lumican	2.89×10^{-2}	2	5	5
41288	Matrix Gla protein	5.58×10^{-4}	−3	7	4
34143	Cholinergic receptor, nicotinic, alpha 1 (muscle)	2.17×10^{-2}	−4	19	17
	Energy metabolism				
M15856	Lipoprotein lipase	6.60×10^{-5}	3	−2	−5
U82818	Uncoupling protein 3 (mitochondrial, proton carrier)	2.14×10^{-3}	−2	nc	−9
AF001787	Uncoupling protein 3 (mitochondrial, proton carrier)	8.52×10^{-4}	−6	nc	−9
	Muscle structure and developmental genes				
J00073	Actin, alpha, cardiac muscle	1.34×10^{-3}	3	7	9
39063	Actin, alpha, cardiac muscle	1.31×10^{-2}	2	7	9
32729	Myosin, heavy polypeptide 3, skeletal, embryonic	2.21×10^{-2}	3	140	124
	Immune response				
J04080	Complement component 1, s subcomponent	3.36×10^{-3}	2	5	3
M65292	H factor (complement)-like 1	4.12×10^{-3}	2	5	3
39409	Complement component 1, r subcomponent	6.63×10^{-3}	2	5	4
32068	Complement component 3a receptor 1	6.21×10^{-3}	−4	22	11
	Intracellular signalling and cell–cell communication				
M62403	Insulin-like growth factor-binding protein 4	6.99×10^{-3}	2	5	4
M38591	S100 calcium-binding protein A10	7.57×10^{-3}	2	5	6
39338	S100 calcium-binding protein A10	2.71×10^{-3}	2	5	6
31924	Soluble adenylyl cyclase	1.07×10^{-2}	−11	−6	−3
	Others and unknown				
Y00339	Carbonic anhydrase II	8.19×10^{-3}	−3	−4	−4
38052	Coagulation factor XIII, A1 polypeptide	2.69×10^{-2}	3	26	11
L11672	Zinc finger protein 91	9.08×10^{-5}	−3	−5	−6
933	Zinc finger protein 91	2.79×10^{-4}	−2	−5	−6
932	Zinc finger protein 91	1.11×10^{-3}	−2	−5	−6
Z49878	Guanidinoacetate N-methyltransferase	7.62×10^{-4}	−2	−4	−3
X96719	C-type lectin, superfamily member 2	1.81×10^{-2}	5	3	4
32057	37 kDa leucine-rich repeat (LRR) protein	3.51×10^{-3}	23	12	nc
1916	v-fos viral oncogene	2.51×10^{-2}	−3	nc	−6

nc = no change in expression level.

cDNA microarray analysis

A cDNA microarray was constructed containing amplicons for 51 genes and ESTs localized to 4q35 and 26 genes and ESTs localized to 10q26, a region containing homologous D4Z4-like subtelomeric repeats. Six FSHD and five normal total muscle RNA samples hybridized independently against the identical internal reference control RNA sample using the constructed microarrays. Results were statistically analyzed to evaluate changes in expression level.

Importantly, we find neither a significant misregulation of 4q35 genes nor a gradient of expression throughout the 4q35 gene region. Relative gene expression levels in FSHD versus normal muscle for all of the characterized genes in 4q35 are listed in Table 5. Fold-changes (FC) range from 0.7 to 1.6 for 4q35 genes, and 0.5–1.9 for the housekeeping genes. Several amplicons from genes found to be dysregulated on the GeneChip (CSRP3, limatin and lumican) were also dysregulated on the cDNA array (3.5–9.5 FC), verifying the potential of this custom array to detect differences in expression levels. All of the cDNA microarray data, including 4q35, 10q26, housekeeping and dysregulated genes and expression values for each of the FSHD and normal muscle samples, can be found as supplementary data on the website www.ucihs.uci.edu/biochem/winokur.

Relative expression levels throughout the 4q35 region are depicted in Figure 2, with closed circles representing characterized, named genes and the open circles corresponding

Table 3. Comparison analysis of affected to unaffected FSHD muscle

SDC	FC	Accession	Gene	Descriptions
A. Increased expression				
12	3.2	D31883	LIMAB1	LIM actin binding protein 1 (limatin)
10.9	**4.2**	**J00073**	**ACTC**	**Actin, alpha, cardiac muscle**
9.9	9.6	M16364	CKB	Creatine kinase, brain
8.8	2.2	X13794	LDHB	Lactate dehydrogenase B
8.7	1.8	M31211	MYL1	Myosin, light polypeptide 1, alkali; skeletal, fast
6.6	3.0	M34309	ERBB3	v-erb-b2 avian erythroblastic leukemia viral oncogene homolog 3
6.6	**2.6**	**V01512**	**FOS**	**v-fos FBJ murine osteosarcoma viral oncogene homolog**
6.6	**1.7**	**M15856**	**LPL**	**Lipoprotein lipase**
B. Decreased expression				
−8.8	**0.6**	**M86407**	**ACTN3**	**Actinin, alpha 3**
−6.6	**0.7**	**Z38133**	**HSMYOSIN**	**Myosin**
−6.6	**0.7**	**AF001787**	**UCP3**	**Uncoupling protein 3**
−6.6	2.4	M12963	ADH1	Alcohol dehydrogenase 1 (class I), alpha polypeptide

Bold denotes transcripts dysregulated in common with other muscular dystrophies. SDC = sum of difference call, described in Materials and Methods.

Table 4. Oligonucleotide (GeneChip) microarray analysis of 4q35 gene expression

Probe set		Gene description	Symbol	HuFL			U95A		
HuFL	U95A			*P*-value	Fold	Obs (C/E)	*P*-value	Fold	Obs (C/E)
D10040	40082	Fatty-acid–coenzyme A ligase, long-chain 1	FACL2	0.021	1.91	6/6	0.489	1.07	6/9
J04982	32822	Adenine nucleotide translocator 1	ANT1/SLC25A4	0.057	1.32	6/6	0.075	1.29	6/9
X15949	1220	Interferon regulatory factor 2	IRF2	0.541	1.16	6/6	0.461	1.09	6/9
L76159	38923	FSHD region gene 1	FRG1	0.524	1.11	6/6	0.630	−1.20	6/9
M13143	32353	Kallikrein B plasma (Fletcher factor) 1	KLKB1	0.456	1.25	6/6	0.934	1.01	5/7
X87241	40454	FAT tumor suppressor (*Drosophila*) homolog	FAT	0.583	1.26	5/6	0.627	1.44	4/8
U13737	36143	Caspase 3, apoptosis-related cysteine protease	CASP3/CPP32	0.294	1.60	5/4	0.853	1.26	5/8
M20218	35591	Coagulation factor XI	F11	0.871	−1.03	6/6	0.064	−21.33	2/0[a]
na	31686	Tubulin, beta polypeptide 4, member Q	TUBB4Q	na	na	na	0.947	1.00	6/8
na	33488	Toll-like receptor 3	TLR3	na	na	na	0.329	−1.27	6/7
na	39690	Alpha-actinin-2-associated LIM protein	ALP	na	na	na	0.316	1.15	6/9
na	39554	Inhibitor of growth family, 1-like	ING1L	na	na	na	0.818	1.03	6/9
na	39295	Arg/Abl-interacting protein	ARGBP2	na	na	na	0.079	−1.9	6/9
na	34423	DKF2P564J102 protein	DKF2P564J102	na	na	na	0.092	3.2	3/2[a]
na	630	dCMP deaminase	DCTD	na	na	na	0.452	−1.2	6/9

[a]Expression values >0 were present in fewer than three samples for each experimental group. Fold change values for these transcripts are therefore not reliable.

to ESTs. The size of each circle reflects significance of observed fold change (smaller *P*-value corresponds to larger circle). Clearly, a gradient does not exist correlating relative expression of 4q35 genes in FSHD versus normal muscle with distance from the telomere. This again is contradictory to the suggestion of a FSHD position effect presented by Gabellini *et al.* (21).

Many FSHD dysregulated genes are direct targets of MyoD

Many of the genes with altered expression patterns in FSHD muscle are early direct targets of MyoD (38). Of the 63 characterized genes identified as direct MyoD targets in primary murine fibroblasts transfected with a MyoD-ER fusion construct, 46 are also represented on the HuFL and U95A arrays used in this study. Of these 46 genes, 11 (24%) are significantly altered in FSHD (Table 6A). In addition to these direct targets of MyoD, many other genes identified in this study directly influence the activity of MyoD and the process of myogenic differentiation. Table 6B lists all significantly altered MyoD target genes from either the HuFL or U95A GeneChips. Each of these genes displayed a greater than 2-fold change in expression level and a *P*-value of <0.05. The complete list of all significantly altered genes, amongst which are the MyoD target genes listed in Table 6B, can be found at www.ucihs.uci.edu/biochem/winokur.

Muscle LIM protein (CSRP3/MLP) is significantly upregulated in FSHD muscle (2.9-fold, $P = 6.9 \times 10^{-7}$ on HuFL array, 2.4-fold, $P = 2.5 \times 10^{-5}$ on U95A array). CSRP3/MLP is a positive regulator of myogenesis, promoting myogenic differentiation through enhancing the activity of MyoD (39). Overexpression of MLP in C2 myoblasts induces myogenic differentiation (26). Another gene with increased expression in FSHD that directly interacts with MyoD is the MyoD family inhibitor MDF1 (40). Four and a half LIM domains 2 (FHL2), another gene involved in myoblast differentiation, is also up-regulated in FSHD muscle. FHL2 is down-regulated during transformation of normal myoblasts to rhabdomyosarcoma cells (41). FHL2 interacts with insulin growth factor receptor 5 (42), a direct target of MyoD also altered in FSHD (38).

Table 5. cDNA microarray analysis of 4q35 gene expression

Gene description	Symbol	FC
4q35 genes		
Fatty-acid–coenzyme A ligase, long-chain 2	FACL2	1.6
Alpha-actinin-2-associated LIM protein	ALP	1.5
FAT tumor suppressor homolog	FAT	1.4
Homo sapiens Arg/Abl-interacting protein A	ARGBP2	1.3
Interferon regulatory factor-2	IRF2	1.3
FSHD region gene 2	FRG2	1.2
Arg/Abl-interacting protein ArgBP2	ARGBP2	1.1
Toll-like receptor-3	TLR3	1.0
Inhibitor of growth family, member 1-like	ING1L	1.0
Hydroxyprostaglandin dehydrogenase 15-(NAD)	HPGD	1.0
Adenine nucleotide translocator-1	ANT	0.9
Coagulation factor XI	FXI	0.9
Adenine nucleotide translocator-1	ANT	0.8
Kallikrein B, plasma (Fletcher factor) 1	KLKB1	0.8
Alternate splice product of ALP	SMT7	0.8
Facioscapulohumeral muscular dystrophy region gene-1	FRG1	0.7
Caspase 3	CPP32	0.7
Facioscapulohumeral muscular dystrophy region gene-1	FRG1	0.7
Melatonin receptor type 1A	MTNR1A	NE
Double homeodomain, D4Z4	DUX4	NE
Housekeeping genes		
Sigma receptor (SR31747 binding protein 1)	SR-BP1	1.9
Major histocompatibility complex, class I, A	HLA-A	1.3
Interleukin enhancer binding factor 2, 45 kDa	ILF2	1.2
Phospholipase A2, group IB	PLA2G1B	1.1
Polymerase (RNA) II (DNA directed) polypeptide K	POLR2K	1.1
Eukaryotic translation elongation factor 1 alpha 1	EEF1A1	1.0
Ubiquitin-conjugating enzyme E2D 2	UBE2D2	1.0
Hypoxanthine phosphoribosyltransferase 1	HPRT1	1.0
Ornithine decarboxylase 1	ODC1	1.0
Tubulin, alpha 1	TUBA1	0.9
Ribosomal protein L37a	RPL37A	0.5
RNA-binding protein S1, serine-rich domain	RNPS1	0.5
Array control genes		
Limatin	ABLIM	9.5
Cysteine and glycine-rich protein 3 (muscle LIM protein)	CSRP3	5.4
Lumican	LUM	3.5

FC = relative RNA expression value in FSHD versus normal muscle. NE = not expressed. For housekeeping and array comparison genes, if two spots were present on array for that transcript, the average relative expression value is given.

Delta-like homolog DLK1, a gene involved in the differentiation of several cell types (43), is also elevated in FSHD. Increased expression of DLK1 has been shown to be responsible for the muscular hypertrophy in callipyge sheep (44) and may be responsible for the abdominal muscular abnormalities in paternal UPD14 (45). The muscular hypertrophy in callipyge sheep is probably due to the inhibitory affect of DLK on differentiation. Delta indirectly regulates the transcription of myogenic target genes such as myocyte enhancer factor 2C (MEF2C) (46). MEF2C is down-regulated in FSHD muscle (Table 5) (47). MEF2C interacts with HDAC4, key regulator of myogenesis, also down-regulated in FSHD muscle (48). HDAC4 itself is regulated through calcium/calmodulin signaling, and may be affected by decrease in calmodulin RNA in FSHD muscle (Table 1).

Other genes found to be dysregulated in FSHD that play key roles in differentiation and accompanying apoptosis include members of the transforming growth factor, caspase and metallothionein families (Table 6B). Myogenesis requires the coordinate regulation of cell cycle withdrawal and enhanced apoptosis (49). Metallothioneins are recruited into the nucleus to protect against free-radical toxicity, oxidative stress and apoptosis (50,51). Both caspase 1 and 2 are elevated in FSHD muscle (Table 6B), while a large number of metallothionein genes are reduced in expression. Indeed, FSHD myoblasts demonstrate an increased vulnerability to oxidative stress (33), which may influence the ability of these cells form fully functional myotubes.

DISCUSSION

The gene expression profiling data presented here suggests an intriguing hypothesis for the pathophysiological basis of FSHD: a primary defect in muscle cell differentiation. Many of the genes dysregulated in FSHD are involved in myogenesis, cellular differentiation and cell-cycle control. Aberrant transcription of genes involved in differentiation and proliferation could either result from an intrinsic defect in FSHD muscle, or result from enhanced regeneration and recruitment of satellite cells in affected muscle. As the majority of these genes are deregulated in an FSHD disease-specific manner, and are not dysregulated in the other muscular dystrophies studied, we propose that some of these expression differences result from a primary differentiation defect in FSHD muscle rather than a result of secondary dystrophic changes. Although the mechanism of gene dysregulation in FSHD remains unknown, the genes mis-expressed in FSHD are highly enriched for genes that interact with, or are direct targets of, MyoD, suggesting an enhancement of an early sub-program of MyoD-mediated muscle cell differentiation.

In support of this hypothesis, FSHD myoblasts in culture are seen to fuse at a faster rate than controls, suggesting that the muscle differentiation program has been turned on at an earlier, perhaps premature timepoint (D. Figlewicz, personal communication) (52). This may be mediated by the up-regulation of cyclin dependent kinase inhibitor protein, p21, in FSHD myoblasts (33,52), also a direct target of MyoD (53). The premature fusion of FSHD myoblasts is not due to replicative senescence of these cells in diseased muscle, as telomeric/centromeric repeat ratios do not differ between FSHD and normal myoblasts (52).

As FSHD is an adult-onset muscular dystrophy, one must also consider the possibility that myogenesis in FSHD results from inefficient termination of the myogenic program once differentiation has occurred. The continued expression of genes involved in differentiation, as seen in this study, may interfere with proper function of muscle in the differentiated state. Interestingly, alteration in D4Z4 copy number has been shown to affect myogenic differentiation in C2C12 myoblasts (54). Deformed myotube morphology and a reduced myotube fusion index result from increasing numbers of D4Z4. While disease is inversely correlated to the number of D4Z4 repeats in FSHD, the demonstration that D4Z4 can affect myogenesis in *trans* is further support for a disruption of this process in FSHD.

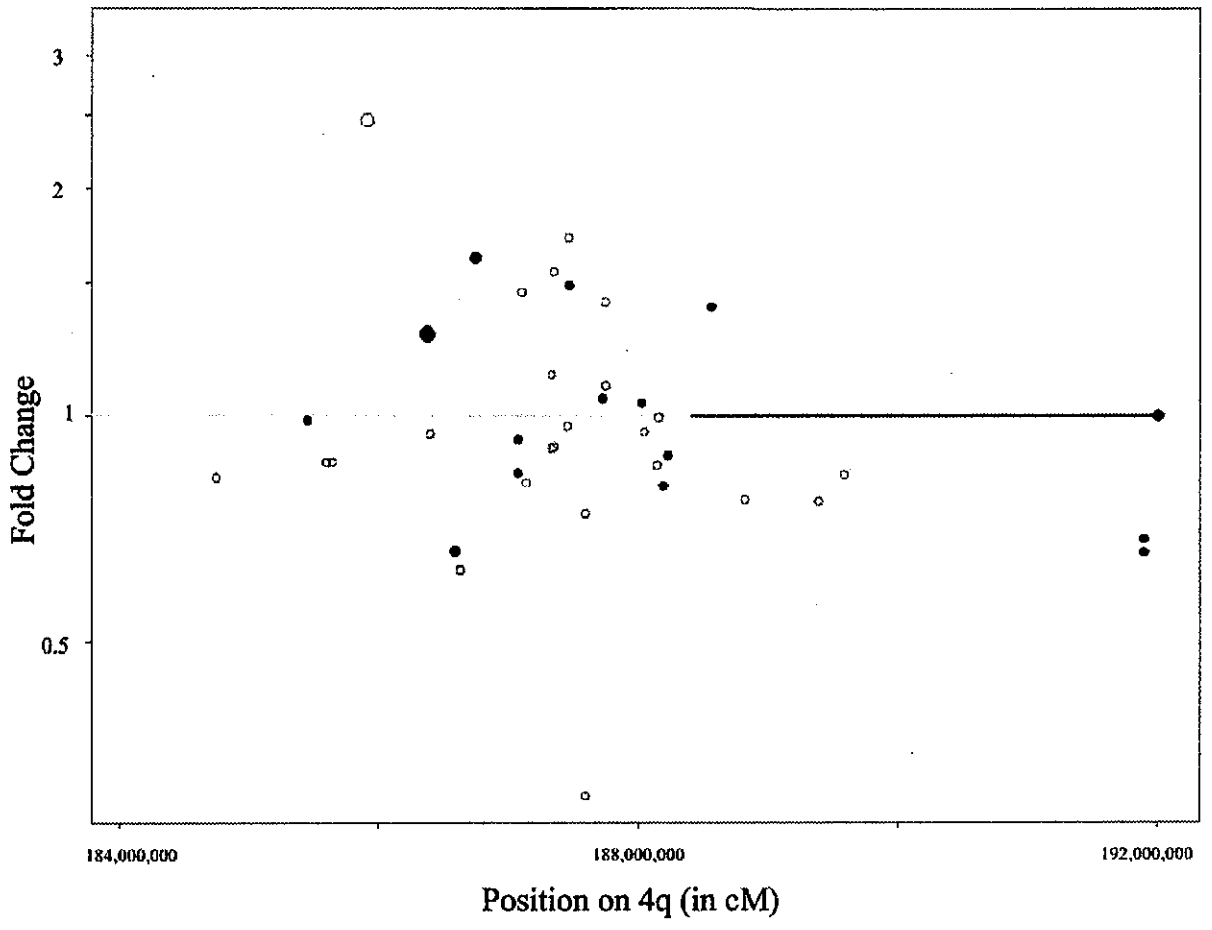

Figure 2. Fold change of 4q35 transcript expression levels in FSHD versus normal muscle using cDNA microarray analysis. Neither a significant misregulation of 4q35 genes nor a gradient of expression throughout 4q35 is noted. Size of each circle reflects significance of observed fold change (smaller *P*-value corresponds to larger circle). Closed circles are characterized, named genes. Open circles correspond to ESTs. The 4q telomere is represented by the far right of the graph.

Although a gradient of altered expression throughout 4q35 has been proposed as part of a position effect model for FSHD (21), our data firmly disputes this. Both oligonucleotide and cDNA microarray analysis do not reveal any evidence for increased expression of 4q35 genes in FSHD muscle. Examination of all single-copy genes on 4q35 (FACL2, ANT1, IRF2, KLKB1, FAT, CPP32, F11, TLR3, ALP, ING1L, ARGBP2, HPGD, DCTD and MTNR1A) does not reveal an aberrant pattern of gene expression. This conclusion is supported by several other studies of 4q35 gene expression. Bouji *et al.* (22) examined the single copy 4q35 gene actinin-associated LIM protein (ALP) in FSHD and normal muscle. No difference in either RNA or protein expression levels of ALP was observed. Van Deutekom *et al.* (23) investigated allele-specific FRG1 steady-state transcript levels using RNA-based single-strand conformation polymorphism (SSCP) analysis. No evidence for a position effect on allelic transcription was obtained in lymphocytes or muscle biopsies from patients and controls. Recent analysis of the single copy 4q35 gene adenine nucleotide translocator (ANT1) as well as FRG1 expression using real-time RT–PCR again did not detect up-regulation of these transcripts in FSHD skeletal muscle tissue (M. Ehrlich and S. van der Maarel, personal communication). All of these studies on 4q35 gene expression, as well as the data we present here, have reached a different conclusion than that reported by Gabellini *et al.* (21). The reason for this discrepancy is as yet unclear.

As the vast majority of expression studies do not support the position effect model for FSHD, we propose an alternate model for FSHD pathogenesis. Alterations in 4q35 subtelomeric chromatin structure may affect the global expression of genes involved in myogenic differentiation rather than a regional disruption of 4q35 genes. Recent data lends strong support to consideration of FSHD as a chromatin disease. A polymorphism of the 4q telomere exists in the population with nearly equal frequencies (12). FSHD is uniquely associated with the 4qA allele variant containing β-satellite, a sequence previously associated with heterochromatin (55). In addition, many D4Z4 CpG methylation sensitive restriction sites are significantly hypomethylated in FSHD patients compared to normal individuals (S. van der Maarel, personal communication) (56).

Table 6. FSHD altered genes that are (A) direct targets of MyoD or (B) involved in myogenic differentiation

Affy accession	Description	Gene	*P*-value	Fold change
A. Direct MyoD targets with altered regulation in FSHD				
158	DnaJ (Hsp40) homolog, subfamily B, member 4	DNAJB4	1.34×10^{-2}	16.2
M55998	Human alpha-1 collagen type I gene, 3′ end	COL1AZ	1.91×10^{-5}	5.4
40863	Creatine kinase, brain	CKB	4.06×10^{-3}	2.7
32648	Delta-like homolog (*Drosophila*)	DLK1	3.15×10^{-5}	2.4
39063	Actin, alpha, cardiac muscle	ACTC	1.31×10^{-2}	2.4
M12963	Alcohol dehydrogenase 1 (class I), alpha polypeptide	ADH1	2.05×10^{-3}	−2.9
M92843	Zinc finger protein homologous to Zfp-36 in mouse	ZFP36	3.15×10^{-3}	−2.9
L27559	Insulin-like growth factor binding protein 5	IGFBP5	3.23×10^{-2}	−3.1
X68505	Myocyte-specific enhancer 2	MEF2	3.22×10^{-2}	−3.3
34143	Cholinergic receptor, nicotinic, alpha polypeptide 1 (muscle)	CHRNA1	2.17×10^{-2}	−3.6
37724	v-myc avian myelocytomatosis viral oncogene homolog	MYC	3.96×10^{-3}	−4.5
B. Additional genes involved in myogenic differentiation				
38156	MyoD family inhibitor	MDFI	3.91×10^{-3}	33.3
574	Caspase 1, apoptosis-related cysteine protease	CASP1	6.44×10^{-4}	10.0
34448	Caspase 2, apoptosis-related cysteine protease	CASP2	8.39×10^{-3}	4.3
1830	Transforming growth factor, beta 1	TGFB1	1.09×10^{-3}	3.6
U49837	Cardiac LIM protein; cysteine- and glycine-rich protein 3	CSRP3	6.87×10^{-7}	2.9
38422	Four and a half LIM domains 2	FHL2	2.60×10^{-3}	2.7
J02621	High-mobility group (nonhistone chromosomal) protein 14	HMG14	4.98×10^{-3}	2.4
32583	v-jun avian sarcoma virus 17 oncogene homolog	JUN	2.97×10^{-3}	−2.0
870	Metallothionein 3 [growth inhibitory factor (neurotrophic)]	MT3	1.23×10^{-3}	−2.1
38374	TGFB inducible early growth response	TIEG	1.79×10^{-3}	−2.2
1767	Transforming growth factor, beta 3	TGFB3	9.38×10^{-3}	−2.3
M69043	Nuclear factor of kappa light gene enhancer in B-cells inhibitor, alp	NFKBIA	5.37×10^{-4}	−2.3
39120	Metallothionein 1L	MT1L	6.97×10^{-5}	−2.6
36130	Metallothionein 1E (functional)	MT1E	3.64×10^{-5}	−2.7
32746	CASP8 and FADD-like apoptosis regulator	CFLAR	1.36×10^{-4}	−2.7
31622	Metallothionein 1F (functional)	MT1F	7.48×10^{-4}	−2.8
38271	Histone deacetylase 4	HDAC4	3.47×10^{-3}	−3.5
32786	Jun B proto-oncogene	JUNB	6.05×10^{-3}	−3.5
39594	Metallothionein 1H	MT1H	1.31×10^{-4}	−3.6
31623	Metallothionein 1A (functional)	MT1A	4.84×10^{-4}	−3.9
39081	Metallothionein 2A	MT2A	4.73×10^{-5}	−5.1
544	Nuclear factor of kappa light gene enhancer in B-cells 2	NFKB2	2.46×10^{-3}	−64.6

However, the differences in chromatin structure are unlikely to act in *cis* (i.e. from a localized position effect), as 4q35 gene expression does not appear to be altered in FSHD muscle. Instead, we propose that FSHD may result from improper nuclear localization. D4Z4 deletions may affect the localization of 4qtel to a nuclear domain in which aberrant gene expression can occur. Appropriate nuclear localization is essential for normal gene expression (57). Telomeric regions are known to localize to discrete nuclear domains and regulate expression of genes within this domain (58,59). As the 4q telomere is one of very few telomeres to localize to the nuclear periphery in myoblasts (our unpublished data), the role of D4Z4 in attachment to the nuclear envelope is an area of active research. Disruption of the nuclear envelope in other forms of neuromuscular disease, such as Emery–Dreifuss muscular dystrophy (EDMD), limb girdle muscular dystrophy (LGMD1B), dilated cardiomyopathy (CMD1A) and autosomal recessive Charcot–Marie–Tooth disease (AR-CMT2) is well established (60,61). Emerin and lamin A/C mutations underlie these disorders, and are thought to be pathogenic either through direct effects on nuclear envelope integrity or through perturbations in tissue-specific gene expression patterns (62). Effects on gene expression may arise through inappropriate methylation status of sequences normally attached to the nuclear envelope or matrix (63,64). Defective DNA replication and cell cycle progression, cellular functions also intimately involved with the nuclear envelope and lamina, may lead to the increased vulnerability to free radical damage seen in FSHD myoblasts.

While precise definition of pathogenetic mechanism responsible for FSHD remains elusive, this study brings together many of the disparate finding on FSHD: altered rates of myoblast fusion and cell cycle progression, enhanced oxidative stress and differential methylation. Many of these findings can now be seen as either the cause or effect of alterations in specific stages of myogenic differentiation. As the specific gene expression changes likely to be responsible for this aberration are not seen in other types of muscular dystrophies, we propose that FSHD exhibits a unique defect in myogenic differentiation. This defect may be related to global effects on gene expression mediated by nuclear localization and alterations in nuclear envelope association rather than a postion effect on 4q35 specific gene expression. Future directions in FSHD should therefore focus on more global analysis of cellular processes such as the cell cycle and the effects of nuclear localization on gene expression of muscle transcripts, and not solely on the identification and analysis of 4q35 specific genes.

MATERIALS AND METHODS

Muscle biopsies

Initially, expression profiling was performed on three sets of matched muscle biopsies (affected and unaffected muscles from three independent FSHD patients) and three normal controls using the HuFL GeneChip. Additional biopsy sets (nine FSHD and six normal controls) were then analyzed on the U95A GeneChip in order to extend and confirm the dysregulation of specific transcripts identified by the HuFL GeneChip. Gene expression profiles were generated comparing both FSHD affected muscle to normal muscle (HuFL and U95A GeneChips), as well as FSHD affected muscle to unaffected muscle (biceps and deltoid, respectively) within three patients (HuFL GeneChips). In order to reduce noise due to *experimental* variability, target cRNA from each biopsy was prepared in replicate, and independently hybridized to one of two HuFL GeneChips for that biopsy sample. In order to reduce noise due to *individual* variability, and to monitor the progression of muscle involvement in FSHD, matched biopsies from individual FSHD patients were used. Thus, a total of nine biopsies were prepared in replicate and hybridized to 18 HuFL GeneChips. The expression profiles were then compared to a series of disease control profiles including Duchenne muscular dystrophy and α-sarcoglycan deficiency (25) using identical RNA isolation methodology and GeneChip formats. No corresponding dataset exists for the FSHD versus normal dataset, although a larger set of muscle (nine FSHD and six normal) were used for the analysis.

cRNA preparation, hybridization and staining. Muscle biopsies were used to extract total RNA by using TRIzol® reagent (GibcoBRL Life Technologies, MD, USA). Each biopsy was divided into two fragments, and RNA isolated from each fragment independently. Ten micrograms of total RNA from each biopsy fragment were converted into double stranded cDNA by using SuperScript Choice system (GibcoBRL Life Technologies, MD, USA) with an oligo-dT primer containing T7 RNA polymerase promoter (Integrated DNA Technologies, Coralville, IA, USA). The double-stranded cDNA was purified with phase lock gel 1 light (5 Prime, Boulder, CO, USA), then used for *in vitro* transcription using the MEGAscript T7 IVT kit (Ambion). Biotin-labeled cRNA was purified by RNeasy kit (Qiagen, CA, USA), and fragmented randomly to approximately 200 bp (200 mM Tris–acetate, pH 8.2, 500 mM KOAc, 150 mM MgOAc). Fifteen micrograms of fragmented cRNA were hybridized to Affymetrix GeneChip HuFL or U95A microarrays for 16 h. The microarray was washed and stained by the Affymetrix Fluidics Station 400, using instructions and reagents provided by Affymetrix. This involves removal of non-hybridized probe, and then incubation with phycoerythrin-streptavidin to detect bound probe. Fluorescent images were read using the Hewlett-Packard G2500A Gene Array Scanner.

Data analysis

Raw expression data, as well as statistical analyses of the data, are posted on the website www.ucihs.uci.edu/biochem/winokur.

Analysis of hybridization intensities for the HuFL and U95A array was performed with GeneChip software Version 3.3 and Version 4, respectively, developed by Affymetrix. Briefly, each gene is queried by perfect-match (PM) probes as well as mismatch (MM) probes with a centrally placed single base change. Comparison of the hybridization signals from the PM and MM probes allows a measure of signal intensity the average difference (AD), and elimination of most non-specific cross-hybridization from the data analysis. Values of intensity difference as well as ratios of each probe pair are used for determination of whether a gene is called 'present' or 'absent'. Quality control (QC) criteria and data for each array, such as internal and hybridization controls, percentage present calls and oligo B2 corner patterns, are posted on the website listed above.

For the comparison of FSHD and normal muscle expression data, AD values for each transcript across all muscle samples were imported into Excel, and output was then analyzed with Cyber T. Cyber T is a statistical program based upon Student's *t*-test which is designed for output data from large-scale microarray experiments (65). Regularized *t*-tests between experimental groups are generated within a Bayesian statistical framework (66). Estimates of variance of expression levels for each gene are therefore improved by including the variance of other genes with similar expression levels. Transcripts were considered to be significantly dysregulated if they displayed a 2-fold or greater fold change and had a Cyber T generated *P*-value ≤ 0.05.

For the comparison of FSHD affected versus unaffected muscle, rather than utilize AD values across all samples, we were interested in comparing expression profiles *within* patients. Thus, each affected sample was prepared in replicate and then compared to each replicate from the unaffected muscle for each patient, yielding a total of 12 pairwise comparisons. For the comparative analysis, a difference call (DC) was made for each transcript when comparing two samples. This DC value was based upon the difference in AD value, as well as the number of probe pairs that either increased or decreased in intensity (increase or decrease ratio). Transcripts were considered significantly dysregulated if they displayed consistent DCs in >40% of all pairwise comparisons and had greater an average fold change of greater than 1.5 across all pairwise comparisons. Such criteria were chosen in part to allow for cross-species comparison of FSHD dysregulated genes to a list of direct MyoD targets (38). The DC were then assigned a numerical value (I = 1, NC = 0, D = −1) for each pairwise comparison. Transcripts were then sorted in Excel according to how consistently they were dysregulated across all FSHD versus normal comparisons by calculating the sum of difference calls (SDC). Expression data from each experiment, as well as complete comparative analyses represented as excel files, and statistical analyses of the data, are posted on the website (http://www.ucihs.uci.edu/biochem/winokur).

Taqman (real-time PCR)

Independent confirmation of select expression changes was performed by real-time RT–PCR (TaqMan) analysis (36). Primers and probes were designed using Primer Express software (PE Applied Biosystems), targeting the terminal 3′

Table 7. TaqMan RT–PCR primers and probes used for expression confirmation

Transcript[a]	Forward primer (5′–3′)	TaqMan probe (5′–3′)	Reverse primer (5′–3′)
CSPR3	GAGAAGGTTATGGGAGGTGGC	AGCCTTGGCACAAGACCTGTTTCCG	CTCTTCCCACAGATGGCACA
DLK	TCACGGACTCTGTGGAGAACC	CATTTGCACCGACGGCTGGGA	CAGGCCCGAACATCTCTATCA
ALP	AGGATGCCGCTCTGTGACA	ACAGCACCAACTATGCCACTCCCACAT	GTACTTATCCCGCGCCTTCA
RNPS1	CCATCTCCTAAGCCCACCAA	TGCACATTGGGAGACTCACCCGG	TCTCCATGATGTGATCCTTGTCA

[a]CSPR3, DLK and ALP probes are FAM-labeled; RNPS1 probe is VIC-labeled.

intron/exon boundary of each transcript to reduce genomic contamination signals (Table 7).

cDNA syntheses, including no-amplification controls, were performed in triplicate using the TaqMan RT Reagents (PE Applied Biosystems), with 1 μg of muscle biopsy total RNA for each 100 μl reaction. TaqMan PCR assays for each amplicon were performed in duplicate in 96-well optical plates on cDNA equivalent to 10 ng of total RNA. Typical 50 μl reactions contained 17 μl dH_2O, 25 μl 2 × Taqman Universal PCR Master Mix (PE Applied Biosystems), 1 μl sense primer (20 uM), 1 μl antisense primer (10 μM), and 1 μl Taqman probe (5 μm), and 5 μl cDNA. Thermal cycling conditions were 2 min at 50°C and 10 min at 95°C, followed by 40 cycles at 95°C for 15 s and 60°C for 1 min. Standard curves for each amplicon were generated using serial dilutions of known quantities of reverse-transcribed skeletal muscle total RNA (Stratagene). Data was collected using the ABI PRISM 7700 Sequence Detection System (PE Applied Biosystems), and relative quantities of initial template for each cDNA sample were extrapolated from the standard curve based on threshold cycle (C_t) values.

Construction of cDNA microarrays

A custom glass slide cDNA array consisting of 107 transcripts was made in order to test the position effect hypothesis for FSHD. The cDNAs included 51 genes and expressed sequence tags (ESTs) mapped to 4q35, 26 genes and ESTs mapped to 10q26, 12 housekeeping genes (37) and 18 miscellaneous genes known to be causative for other types of muscular dystrophy or dysregulated according to FSHD muscle GeneChip analysis. The selection of 4q35 and 10q26 ESTs was based on known regional genes and exhaustive Unigene (http:Unigene) database searches to include as complete a set of ESTs as possible at the time the array was constructed. cDNA clones (IMAGE consortium, Research Genetics), preferably with inserts about 1 kb in length and near the 3′ end of the cDNA, were amplified with vector primers and column resin purified. For those genes unavailable from the IMAGE consortium or for which clonal amplification failed, appropriate primers were made based on the known gene sequence, and the product was PCR amplified from cDNA library templates. All amplicons were sequence-verified with a PRISM 377 DNA Sequencer (Applied Biosystems) and examined by agarose gel electrophoresis and spectrophotometry to insure the quality and identity of the products. The cDNA amplicons were diluted to 1 μg/μl in spotting solution M1435 (Sigma) and arrayed onto CMT-GAPS slides (Corning) using an OmniGrid arrayer (GeneMachines). The spot diameter was 120 μm. Each cDNA was represented in duplicate on the microarray, and the housekeeping genes were represented four times each. After plotting, slides were baked at 80°C for 3 h.

Probe hybridization

Labeling was carried out using the NEN Micromax TSA Labeling and Detection Kit (Perkin Elmer Life Sciences, Boston, MA, USA). RT–PCR was performed with 2 μg of total RNA using the fluorescein nucleotide reaction mix. For all slides, RT–PCR was also performed on 2 μg of Universal RNA (Stratagene) using the biotin reaction mix for use as an internal reference control on each slide. RT–PCR was performed for 2 h at 42°C. cDNA was isolated by isopropanol precipitation and resuspended together in TSA kit hybridization buffer Q. All slides were prehybridized by heating in a 5 × SSC, 0.1% SDS, 0.1% BSA solution at 42°C for 45 min, then rinsed in water and isopropanol. The hybridization mixture was denatured and then hybridized to the slides overnight in a 64°C oven in a hydrated hybridization chamber (Corning Life Sciences). Slides were washed and incubated with anti-Fl-HRP followed by Cy3-tyramide to deposit Cy3. They were then washed and incubated with streptavidin-HRP followed by Cy5-tyramide to deposit Cy5.

cDNA microarray detection and quantification

Slides were scanned using a Scanarray 4000 XL scanner (GSI Lumonics) using a 550 nm laser for Cy3 and 649 nm for Cy5. Multiple scans were made for each slide using increasing laser intensities, in order to include bright signals which quickly saturate the scanner as well as weak signals which only appear at high laser intensities. The images were quantified using the Dapple program (http:Dapple), which provides both a reading of the signal intensity of a spot and a judgment of the quality of the identified spot. Spots having a very low intensity or intensity near the scanner's maximum were excluded. Only spots simultaneously deemed acceptable on both the Cy3 and Cy5 image were used. A Cy3/Cy5 intensity ratio was calculated for each accepted spot pair. For each scan of a slide, the spot intensity ratios were normalized by dividing the measured intensity ratios by the median of the measured housekeeping gene intensity ratios of that scan. The log value of this ratio was calculated to produce a normalized log ratio (NLR). A single NLR value for each spot on the slide was made by taking the median of the acceptable NLRs on all scans of the spot (spots appearing on less than two of the scans were rejected). A single NLR was assigned to each transcript on a slide by taking the median of values for redundant spots of that transcript. Finally, FSHD slides were compared to the normal slides. Within groups, only transcripts for which at least half different slides provided a NLR value were included. The median NLR for

each transcript within the FSHD group was divided by the corresponding median value within the normal group, providing a fold change of the transcript expression level. Confidence was evaluated using the Wilcoxon rank sum test.

ACKNOWLEDGEMENTS

Our deepest gratitude goes to the now deceased Dr Kiichi Arahata for his enthusiasm, expertise and collaborative spirit. His presence is greatly missed by all members of the FSHD community. We wish to thank Drs Ko Sahashi (Aichi Medical University) and Masanori Nakagawa (Kyoto Prefectural University of Medicine) for their contribution of muscle biopsy specimens for this study. This study was funded by grants from the MDA (S.T.W.), FSH Society, Inc. (S.T.W. and K.M.F.) and NIH (S.T.W., Y.-W.C.). Additional support was generously provided by the FischerShaw Foundation.

REFERENCES

1. Tawil, R., Figlewicz, D.A., Griggs, R.C. and Weiffenbach, B. (1998) Facioscapulohumeral dystrophy: a distinct regional myopathy with a novel molecular pathogenesis. *Ann. Neurol.*, **43**, 279–282.
2. Padberg, G. and Adams, C. (2000) Facioscapulohumeral muscular dystrophy. In Pulst, S.-M. (ed.), *Neurogenetics*. Oxford University Press, Oxford, pp. 105–116.
3. Padberg, G.W., Brouwer, O.F., de Keizer, R.J.W., Gruter, A.M., Wijmenga, C., Grote, J.J. and Frants, R.R. (1992) Retinal vascular disease and sensorineural deafness are part of facioscapulohumeral muscular dystrophy. *Am. J. Hum. Genet.*, **51** (S), A104.
4. Funakoshi, M., Goto, K. and Arahata, K. (1998) Epilepsy and mental retardation in a subset of early onset 4q35-facioscapulohumeral muscular dystrophy. *Neurology*, **50**, 1791–1794.
5. Arahata, K., Ishihara, T., Fukunaga, H., Orimo, S., Lee, J.H., Goto, K. and Nonaka, I. (1995) Inflammatory response in facioscapulohumeral muscular dystrophy (FSHD): immuno-cytochemical and genetic analyses. *Muscle Nerve*, **2**, S56–66.
6. Padberg, G.W., Frants, R.R., Brouwer, O.F., Wijmenga, C., Bakker, E. and Sandkuijl, L.A. (1995) Facioscapulohumeral muscular dystrophy in the Dutch population. *Muscle Nerve*, **2**, S81–84.
7. Zatz, M., Marie, S.K., Passos-Bueno, M.R., Vainzof, M., Campiotto, S., Cerqueira, A., Wijmenga, C., Padberg, G. and Frants, R.R. (1995) High proportion of new mutations and possible anticipation in Brazilian facioscapulohumeral muscular dystrophy families. *Am. J. Hum. Genet.*, **56**, 99–105.
8. Lunt, P.W., Compston, D.A. and Harper, P.S. (1989) Estimation of age dependent penetrance in facioscapulohumeral muscular dystrophy by minimising ascertainment bias. *J. Med. Genet.*, **26**, 755–760.
9. Wijmenga, C., Hewitt, J.E., Sandkuijl, L.A., Clark, L.N., Wright, T.J., Dauwerse, H.G., Gruter, A.M., Hofker, M.H., Moerer, P., Williamson, R. and Frants, R.R. (1992) Chromosome 4q DNA rearrangements associated with facioscapulohumeral muscular dystrophy. *Nat. Genet.*, **2**, 26–30.
10. van Deutekom, J.T., Wijmenga, C., van Tienhoven, E.A.E., Gruter, A.-M., Hewitt, J.E., Padberg, G.W., van Ommen, G.-J.B., Hofker, M.H. and Frants, R.R. (1993) FSHD associated DNA rearrangements are due to deletions of integral copies of a 3.2 kb tandemly repeated unit. *Hum. Mol. Genet.*, **2**, 2037–2042.
11. Hewitt, J.E., Lyle, R., Clark, L.N., Valleley, E.M., Wright, T.J., Wijmenga, C., van Deutekom, J.C., Francis, F., Sharpe, P.T., Hofker, M. *et al.* (1994) Analysis of the tandem repeat locus D4Z4 associated with facioscapulohumeral muscular dystrophy. *Hum. Mol. Genet.*, **3**, 1287–1295.
12. van Geel, M., Dickson, M.C., Beck, A.F., Bolland, D.J., Frants, R.R., van der Maarel, S.M., de Jong, P.J. and Hewitt, J.E. (2002) Genomic analysis of human chromosome 10q and 4q telomeres suggests a common origin. *Genomics*, **79**, 210–217.
13. Bengtsson, U., Altherr, M.R., Wasmuth, J.J. and Winokur, S.T. (1994) High resolution fluorescence in situ hybridization to linearly extended DNA visually maps a tandem repeat associated with facioscapulohumeral muscular dystrophy immediately adjacent to the telomere of 4q. *Hum. Mol. Genet.*, **3**, 1801–1805.
14. Gabriels, J., Beckers, M.C., Ding, H., De Vriese, A., Plaisance, S., van der Maarel, S.M., Padberg, G.W., Frants, R.R., Hewitt, J.E., Collen, D. and Belayew, A. (1999) Nucleotide sequence of the partially deleted D4Z4 locus in a patient with FSHD identifies a putative gene within each 3.3 kb element. *Gene*, **236**, 25–32.
15. Winokur, S.T., Bengtsson, U., Feddersen, J., Mathews, K.D., Weiffenbach, B., Bailey, H., Markovich, R.P., Murray, J.C., Wasmuth, J.J., Altherr, M.R. and Schutte, B.C. (1994) The DNA rearrangement associated with facioscapulohumeral muscular dystrophy involves a heterochromatin-associated repetitive element: implications for a role of chromatin structure in the pathogenesis of the disease. *Chromosome Res.*, **2**, 225–234.
16. Lyle, R., Wright, T.J., Clark, L.N. and Hewitt, J.E. (1995) The FSHD-associated repeat, D4Z4, is a member of a dispersed family of homeobox-containing repeats, subsets of which are clustered on the short arms of the acrocentric chromosomes. *Genomics*, **28**, 389–397.
17. Qumsiyeh, M.B. (1999) Structure and function of the nucleus: anatomy and physiology of chromatin. *Cell Mol. Life Sci.*, **8**, 1129–1140.
18. Parseghian, M.H., Newcomb, R.L., Winokur, S.T. and Hamkalo, B.A. (2000) The distribution of somatic H1 subtypes is nonrandom on active vs inactive chromatin. *Chromosome Res.*, **8**, 405–424.
19. Tsien, F., Sun, B., Hopkins, N.E., Vedanarayanan, V., Figlewicz, D.A., Winokur, S.T. and Ehrlich, M. (2000) Hypermethylation of the FSHD syndrome-associated D4Z4 repeat in normal and FSHD somatic cell populations but not in ICF syndrome cells. *Mol. Genet. Metab.*, **74**, 322–331.
20. Lemmers, R.J., van der Maarel, S.M., van Deutekom, J.C., van der Wielen, M.J., Deidda, G., Dauwerse, H.G., Hewitt, J., Hofker, M., Bakker, E., Padberg, G.W. and Frants, R.R. (1998) Inter- and intrachromosomal sub-telomeric rearrangements on 4q35: implications for facioscapulohumeral muscular dystrophy (FSHD) aetiology and diagnosis. *Hum. Mol. Genet.*, **7**, 1207–1214.
21. Gabellini, D., Green, M.R. and Tupler, R. (2002) Inappropriate gene activation in FSHD: a repressor complex binds a chromosomal repeat deleted in dystrophic muscle. *Cell*, **10**, 339–348.
22. Bouju, S., Pietu, G., Le Cunff, M., Cros, N., Malzac, P., Pellissier, J.F., Pons, F., Leger, J.J., Auffray, C. and Dechesne, C.A. (1999) Exclusion of muscle specific actinin-associated LIM protein (ALP) gene from 4q35 facioscapulohumeral muscular dystrophy (FSHD) candidate genes. *Neuromusc. Disord.*, **9**, 3–10.
23. van Deutekom, J.C., Lemmers, R.J., Grewal, P.K., van Geel, M., Romberg, S., Dauwerse, H.G., Wright, T.J., Padberg, G.W., Hofker, M.H., Hewitt, J.E. and Frants, R.R. (1996) Identification of the first gene (FRG1) from the FSHD region on human chromosome 4q35. *Hum. Mol. Genet.*, **5**, 581–590.
24. Lipshutz, R.J., Fodor, S.P., Gingeras, T.R. and Lockhart, D.J. (1999) High density synthetic oligonucleotide arrays. *Nat. Genet.*, **21**, 20–24.
25. Chen, Y.-W., Zhao, P., Borup, R. and Hoffman, E.P. (2000) Expression profiling in the muscular dystrophies: identification of novel aspects of molecular pathophysiology. *J. Cell Biol.*, **151**, 1321–1336.
26. Arber, S., Halder, G. and Caroni, P. (1994) Muscle LIM protein, a novel essential regulator of myogenesis, promotes myogenic differentiation. *Cell*, **79**, 221–231.
27. Laborda, J. (2000) The role of the epidermal growth factor-like protein dlk in cell differentiation. *Histol. Histopath.*, **15**, 119–129.
28. Igarashi, M., Nagata, A., Jinno, S., Suto, K. and Okayama, H. (1991) Wee1(+)-like gene in human cells. *Nature*, **353**, 80–83.
29. Chen, G. and Quinn, L.S. (1992) Partial characterization of skeletal myoblast mitogens in mouse crushed muscle extract. *J. Cell. Physiol.*, **153**, 563–574.
30. Trommsdorff, M., Gotthardt, M., Hiesberger, T., Shelton, J., Stockinger, W., Nimpf, J., Hammer, R.E., Richardson, J.A. and Herz, J. (1999) Reeler/Disabled-like disruption of neuronal migration in knockout mice lacking the VLDL receptor and ApoE receptor 2. *Cell*, **97**, 689–701.
31. Nakada, Y., Taniura, H., Uetsuki, T., Inazawa, J. and Yoshikawa, K. (1998) The human chromosomal gene for necdin, a neuronal growth suppressor, in the Prader–Willi syndrome deletion region. *Gene*, **213**, 65–72.

32. Junn, E., Han, S.H., Im, J.Y., Yang, Y., Cho, E.W., Um, H.D., Kim, D.K., Lee, K.W., Han, P.L., Rhee, S.G. and Choi, I. (2000) Vitamin D3 up-regulated protein 1 mediates oxidative stress via suppressing the thioredoxin function. *J. Immunol.*, **164**, 6287–6295.
33. Winokur, S.T., Barrett, K., Martin, J.H., Forrester, J.R., Simon, M., Tawil, R., Chung, S.-A., Masny, P.S. and Figlewicz, D.A. (2003) Facioscapulohumeral muscular dystrophy (FSHD) myoblasts demonstrate increased susceptibility to oxidative stress. *Neuromusc. Disord.*, **13**, 322–333.
34. Apostolova, M.D., Ivanova, I.A. and Cherian, M.G. (1999) Metallothionein and apoptosis during differentiation of myoblasts to myotubes: protection against free radical toxicity. *Toxicol. Appl. Pharmac.*, **159**, 175–184.
35. Medhurst, A.D., Harrison, D.C., Read, S.J., Campbell, C.A., Robbins, M.J. and Pangalos, M.N. (2000) The use of TaqMan RT–PCR assays for semiquantitative analysis of gene expression in CNS tissues and disease models. *J. Neurosci. Meth.*, **98**, 9–20.
36. Xia, H., Winokur, S.T., Kuo, W.L., Altherr, M.R. and Bredt, D.S. (1997) Actinin-associated LIM protein: identification of a domain interaction between PDZ spectrin-like repeat motifs. *J. Cell Biol.*, **139**, 507–515.
37. Warrington, J.A., Nair, A., Mahadevappa, M. and Tsyganskaya, M. (2000) Comparison of human adult and fetal expression and identification of 535 housekeeping/maintenance genes. *Physiol. Genomics.*, **2**, 143–157.
38. Bergstrom, D.A., Penn, B.H., Strand, A., Perry, R.L., Rudnicki, M.A. and Tapscott, S.J. (2002) Promoter-specific regulation of MyoD binding and signal transduction cooperate to pattern gene expression. *Mol. Cell*, **9**, 587–600.
39. Kong, Y., Flick, M.J., Kudla, A.J. and Konieczny, S.F. (1997) Muscle LIM protein promotes myogenesis by enhancing the activity of MyoD. *Mol. Cell. Biol.*, **17**, 4750–4760.
40. Chen, C.M., Kraut, N., Groudine, M. and Weintraub, H. (1996) I-mf, a novel myogenic repressor, interacts with members of the MyoD family. *Cell*, **86**, 731–741.
41. Genini, M., Schwalbe, P., Scholl, F.A., Remppis, A., Mattei, M.-G. and Schafer, B.W. (1997) Subtractive cloning and characterization of DRAL, a novel LIM-domain protein down-regulated in rhabdomyosarcoma. *DNA Cell Biol.*, **16**, 433–442.
42. Amaar, Y.G., Thompson, G.R., Linkhart, T.A., Chen, S.T., Baylink, D.J. and Mohan, S. (2002) Insulin-like growth factor-binding protein 5 (IGFBP-5) interacts with a four and a half LIM protein 2 (FHL2). *J. Biol. Chem.*, **277**, 12053–12060.
43. Ruiz-Hidalgo, M.J., Gubina, E., Tull, L., Baladron, V. and Laborda, J. (2002) dlk modulates mitogen-activated protein kinase signaling to allow or prevent differentiation. *Exp. Cell Res.*, **274**, 178–188.
44. Charlier, C., Segers, K., Karim, L., Shay, T., Gyapay, G., Cockett, N. and Georges, M. (2001) The callipyge mutation enhances the expression of coregulated imprinted genes in *cis* without affecting their imprinting status. *Nat. Genet.*, **27**, 367–369.
45. Kurosawa, K., Sasaki, H., Sato, Y., Yamanaka, M., Shimizu, M., Ito, Y., Okuyama, T., Matsuo, M, Imaizumi, K., Kuroki, Y. and Nishimura, G. (2002) Paternal UPD14 is responsible for a distinctive malformation complex. *Am. J. Med. Genet.*, **110**, 268–272.
46. Wilson-Rawls, J., Molkentin, J.D., Black, B.L. and Olson, E.N. (1999) Activated notch inhibits myogenic activity of the MADS-Box transcription factor myocyte enhancer factor 2C. *Mol. Cell. Biol.*, **19**, 2853–2862.
47. Tupler, R., Perini, G., Pellegrino, M.A. and Green, M.R. (1999) Profound misregulation of muscle-specific gene expression in facioscapulohumeral muscular dystrophy. *Proc. Natl Acad. Sci. USA*, **96**, 12650–12654.
48. McKinsey, T.A., Zhang, C.L., Lu, J. and Olson, E.N. (2000) Signal-dependent nuclear export of a histone deacetylase regulates muscle differentiation. *Nature*, **408**, 106–111.
49. Sandri, M. and Carraro, U. (1999) Apoptosis of skeletal muscles during development and disease. *Int. J. Biochem. Cell Biol.*, **31**, 1373–1390.
50. Coyle, P., Philcox, J.C., Carey, L.C. and Rofe, A.M. (2002) Metallothionein: the multipurpose protein *Cell. Mol. Life Sci.*, **59**, 627–647.
51. Cherian, M.G. and Apostolova, M.D. (2002) Nuclear localization of metallothionein during cell proliferation and differentiation. *Cell. Mol. Biol.*, **46**, 347–356.
52. Figlewicz, D.A., Sowden, J.E., Haefele, A., Forrester, J.R., Barrett, K., Kaveic, V. and Tawil, R. (2002) Facioscapulohumeral dystrophy: premature activation of the myogenic program? *FSH International Consortium Workshop*, 14 October, 2003, Baltimore, MD.
53. Otten, A.D., Firpo, E.J., Gerber, A.N., Brody, L.L., Roberts, J.M. and Tapscott, S.J. (1997) Inactivation of MyoD-mediated expression of p21 in tumor cell lines. *Cell Growth Differ.*, **8**, 1151–1160.
54. Yip, D.J. and Picketts, D.J. (2003) Increasing D4Z4 repeat copy number compromises C2C12 myoblast differentiation. *FEBS Lett.*, **537**, 133–138.
55. Lemmers, R.J.L.F., de Kievit, P., Sandkuijl, L., Padberg, G.W., van Ommen, G.J.B., Frants, R.R. and van der Maarel, S.M. (2002) Facioscapulohumeral muscular dystrophy is uniquely associated with one of the two variants of the 4q subtelomere. *Nature Genet.*, **32**, 235–236.
56. Van Overveld, P.G.M., Lemmers, R.J.F., Sandkuijl, L.A., Enthoven, L., Winokur, S.T., Bakels, F., Padberg, G.W., van Ommen, G.-J.B., Frants, R. and van der Maarel, S.M. (2003) D4Z4 hypomethylation in 4q-linked FSHD and non 4q-linked FSHD. *Nat. Genet.* (in press).
57. Cremer, T. and Cremer, C. (2001) Chromosome territories, nuclear architecture and gene regulation in mammalian cells. *Nat. Rev. Genet.*, **2**, 292–301.
58. Baur, J.A., Zou, Y., Shay, J.W. and Wright, W.E. (2001) Telomere position effect in human cells. *Science*, **292**, 2075–2077.
59. Galy, V., Olivo-Marin, J.C., Scherthan, H., Doye, V., Rascalou, N. and Nehrbass, U. (2000) Nuclear pore complexes in the organization of silent telomeric chromatin. *Nature*, **403**, 108–112.
60. Burke, B. and Stewart, C.L. (2002) Life at the edge: the nuclear envelope and human disease. *Nat. Rev. Mol. Cell Biol.*, **3**, 575–585.
61. Ostlund, C. and Worman, H.J. (2003) Nuclear envelope proteins and neuromuscular diseases. *Muscle Nerve*, **27**, 393–406.
62. Hutchison, C.J. (2002) Lamins: building blocks or regulators of gene expression? *Nat. Rev. Mol. Cell. Biol.*, **3**, 848–858.
63. Forrester, W.C., Fernandez, L.A. and Grosschedl, R. (1999) Nuclear matrix attachment regions antagonize methylation-dependent repression of long-range enhancer–promoter interactions. *Genes Dev.*, **13**, 3003–3014.
64. Stratling, W.H. and Yu, F. (1999) Origin and roles of nuclear matrix proteins. Specific functions of the MAR-binding protein MeCP2/ARBP. *Crit. Rev. Eukaryot. Gene Expr.*, **9**, 311–318.
65. Long, A.D., Mangalam, H.J., Chan, Y., Tolleri, L., Hatfield, G.W. and Baldi, P. (2001) Improved statistical inference from DNA microarray data using analysis of variance and a Bayesian statistical framework. Analysis of global gene expression in *Escherichia coli* K12. *J. Biol. Chem.*, **276**, 19937–19944.
66. Baldi, P. and Hatfield, G.W. (2002) Improved statistical inference from DNA array data using a Bayesian statistical framework. In *DNA Microarrays and Gene Expression*. Cambridge University Press, Cambridge, pp. 109–119.

CME

Fukutin-related protein gene mutated in the original kindred limb-girdle MD 2I

A. Driss, PhD; S. Noguchi, PhD; R. Amouri, PhD; M. Kefi, MD; T. Sasaki, MSc; K. Sugie, MD, PhD; S. Souilem, PhD; Y.K. Hayashi, MD; N. Shimizu, PhD; S. Minoshima, PhD; J. Kudoh, PhD; F. Hentati, MD; and I. Nishino, MD, PhD

Abstract—The authors mapped an autosomal recessive form of limb-girdle MD on chromosome 19q13.3 (LGMD2I), further narrowed down the candidate region to 1.1 Mb, and identified one new homozygous mutation in the fukutin-related protein (FKRP) gene on patients of the original Tunisian family. Immunohistochemical and immunoblot analysis showed abnormal expression of α-dystroglycan and laminin-α2 supporting the hypothesis that *FKRP* has a role in the interaction between the extracellular matrix components.

NEUROLOGY 2003;60:1341–1344

Limb-girdle muscular dystrophies constitute a genetically heterogeneous group of disorders. They can be either autosomal dominant (LGMD1) or autosomal recessive (LGMD2). These two groups are further subdivided according to their gene loci.[1] The causative genes encode different classes of proteins, including sarcolemmal, sarcoplasmic, nuclear membrane proteins, and muscle-specific enzymes. The severity and age at onset vary between the types, and even between patients with the same subtype. In addition, some LGMDs can have more than one phenotype.[2]

We have reported a new type of LGMD2, LGMD2I, in a large consanguineous Tunisian family.[3] Symmetric weakness and wasting involving the proximal muscles of all four limbs characterize the clinical features, with a marked predominance of weakness and wasting in the pelvic girdle followed by shoulder and proximal upper limb muscles. In this family, no brain or heart involvement was found. The serum CK level was elevated especially in the early stage of the disease. Muscle biopsy showed dystrophic features with necrotic foci, regenerating fibers, and an increase in connective tissue. Genetic linkage analysis showed a maximum lod score of 4.36 at θ = zero for the microsatellite marker D19S606, mapping the disease locus to chromosome 19q13.3. The recombination events between siblings limited the candidate region to 9 cM between the microsatellite markers D19S412 and D19S879.[3]

To search the gene responsible for LGMD2I, we further narrowed down the candidate region to a 1.1 Mb using new polymorphic markers. This narrowed candidate region contains several candidate genes including fukutin-related protein (*FKRP*) gene, which was recently shown to be mutated in a form of congenital MD, MDC1C,[4] and a milder form of LGMD.[5] To determine if *FKRP* gene is also responsible for LGMD2I in our original Tunisian family, we performed sequence analysis of *FKRP* gene and examined the immunohistochemical expression and

Additional material related to this article can be found on the *Neurology* Web site. Go to www.neurology.org and scroll down the Table of Contents for the April 22 issue to find the title link for this article.

See also pages 1230 & 1246

From the Department of Neuromuscular Research (Drs. Driss, Noguchi, Sugie, Hayashi, and Nishino), National Institute of Neuroscience, National Center of Neurology and Psychiatry NCNP, Kodaira, Tokyo, Japan; the Department of Neurology (Drs. Driss, Amouri, Kefi, Souilem, and Hentati), National Institute of Neurology, La Rabta, Tunis, Tunisia; and the Department of Molecular Biology (Drs. Sasaki, Minoshima, Kudoh, and Shimizu) Keio University School of Medicine, Tokyo, Japan.

Supported by the Uehara Memorial foundation, the Research Grant (14B-4) for Nervous and Mental Disorders from the Ministry of Health, Labor and Welfare of Japan and a fund for the Research for the Future Program from the Japan Society for the Promotion of Science (JSPS) and the Ministry of Education, Culture, Sports, Science and Technology (MEXT) of Japan.

Received November 12, 2002. Accepted in final form February 20, 2003.

Address correspondence and reprint requests to Dr. Adel DRISS, National Center of Neurology and Psychiatry, NCNP, National Institute of Neuroscience, 4-1-1 Ogawa Higashi, Kodaira, 187-8502 Tokyo, Japan; e-mail: adel@weboris.com

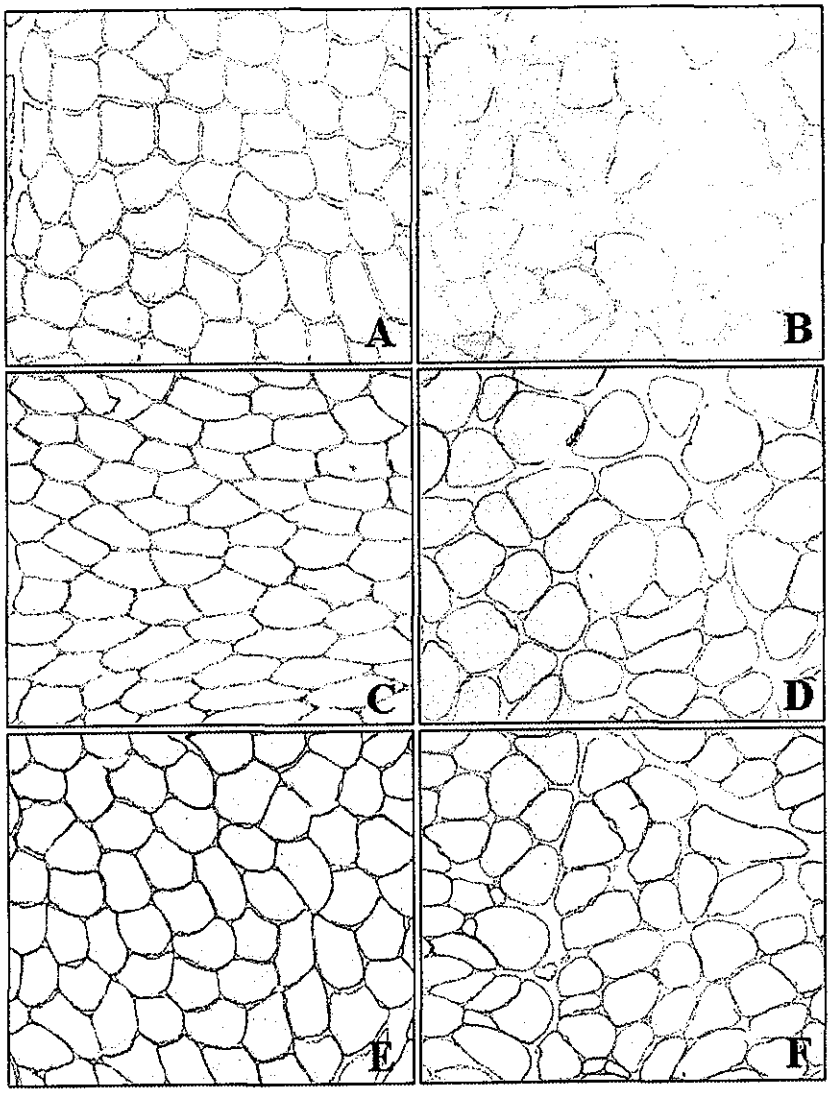

Figure 1. Immunohistochemical localization of α-dystroglycan (A and B), β-dystroglycan (C and D) and laminin-α2 (80-kDa fragment) (E and F) in control (A, C, & E) and patient (B, D, & F) skeletal muscle biopsies. The α-dystroglycan is markedly reduced on most fibers. β-dystroglycan and laminin-α2 stains seem similar to the control.

immunoblot analysis of sarcolemmal proteins including dystroglycans and laminin-α2.

Materials and methods. We studied the consanguineous Tunisian family that we previously reported.[3] This family includes 13 patients. All are related and originally from the same geographic region in southeast Tunisia. Diagnosis was based on clinical examination, course of the disease, family history, and serum CK levels. We performed *bicep* bracii muscle biopsies on 12 patients, and blood samples were collected after informed consent.

We determined the entire genomic sequence of the candidate region by screening genomic DNA databases and constructing a contig of clones. We tested new polymorphic markers within the LGMD2I candidate region.

We amplified the 1.4 kb ORF of the *FKRP* gene by RT-PCR from RNA extracted from a muscle biopsy of one patient and confirmed the mutation in genomic DNA from other affected individuals, their parents, and relatives by direct sequencing. Sequencing reactions were carried out with the primers previously reported[5] and others newly designed.

For immunohistochemical studies, the antibodies used were as follows: monoclonal antibodies against α-dystroglycan (VIA4-1; Upstate Biotechnology, Lake Placid, NY), β-dystroglycan (43DAG1/8D5; Novocastra Laboratories Ltd, Newcastle upon Tyne, UK) and 80-kDa fragment of laminin-α2 (5H2; Chemicon, Temecula, CA). For immunoblot analysis, we used an additional anti-rabbit polyclonal antibody directed against the 300-kDa fragment of the laminin-α2. Frozen muscle biopsy samples were dissected, homogenized in a SDS-based buffer, and separated on a SDS–PAGE gel after heat denaturation. Muscle samples were then transferred to a polyvinyl difluoride membrane and reacted with antibodies.

Results. Initial linkage studies in our family located the candidate region to a 9 cM region between D19S412 and D19S879.[3] Haplotype analysis using new polymorphic markers showed one recombination fraction that cutoff approximately 2.7 cM leading to a 6.7 cM final candidate region between D19S412 and D19S902. After constructing the physical map of this candidate region, the distance between these markers was approximately 1.5 Mb. New polymorphic microsatellite markers further excluded a 0.4 Mb, giving a final candidate region of 1.1 Mb (data not shown).

Recently, *FKRP* gene mutations were reported to be associated with a severe congenital MD, MDC1C,[4] and a mild LGMD.[5] This gene is present within the LGMD2I candidate region and appears to be an excellent candidate gene for our original LGMD2I family. Sequencing this gene revealed two homozygous variations, 341C>G (A114G) and 1486T>A (X496R), on this gene. Parents and some healthy relatives were found heterozygous for both variants. We tested by enzyme restriction and SSCP up to 170 chromosomes from the Tunisian population for these variations to determine which of them is pathogenic. We found four chromosomes having the 341C>G change including one individual in a

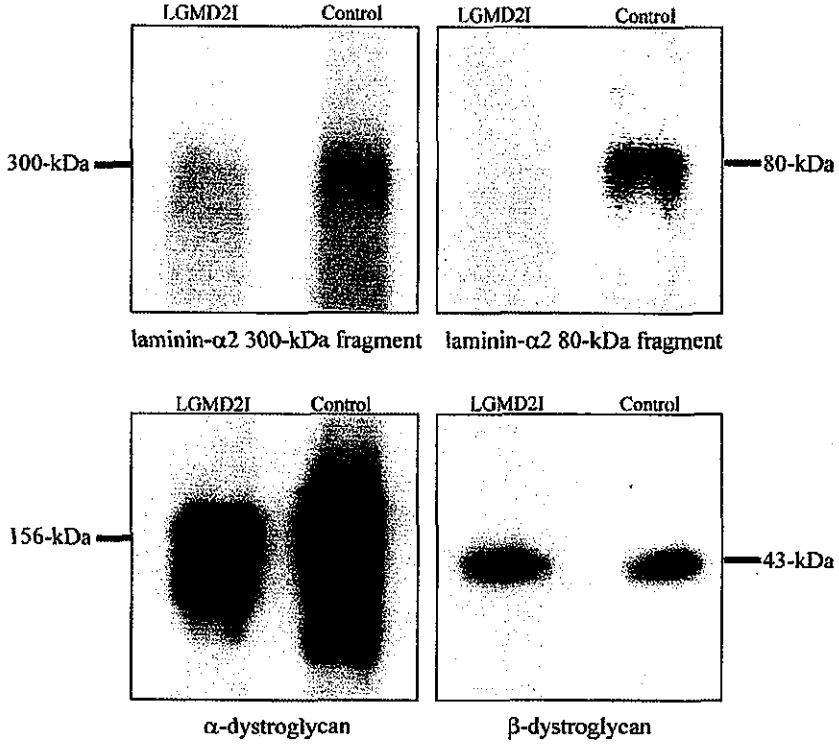

Figure 2. Immunoblot analysis of muscle proteins extracted from LGMD2I patients and controls. The blots show a marked reduction of the α-dystroglycan but not the β-dystroglycan. A reduction of the 300-kDa fragment of the laminin-α2 chain and a virtual-absence of the 80-kDa fragment was observed in the patients.

homozygous state. We did not detect any 1486T>A mutation on the controls. This mutation abolishes the STOP codon and is predicted to add 21 amino acids at the C-terminal end (see figure [E]1 on www.neurology.org).

Immunohistochemical analysis showed a normal expression of the following proteins in muscle fibers: dystrophin, sarcoglycan subunits, sarcospan, utrophin, dysferlin, caveolin-3, dystrobrevin, and collagen IV and VI (data not shown). α-Dystroglycan staining was markedly reduced compared with that in controls while immunoreactivity to β-dystroglycan was preserved. No special reduction of sarcolemmal labeling was seen when immunostained with the antibodies against the 80-kDa fragment of laminin-α2 (figure 1). These findings were verified on five different patients' biopsies. Even though the samples were obtained at different clinical stages and different ages, all presented a similar reduction of the α-dystroglycan.

Immunoblot analysis of the α-dystroglycan showed a broad-band spanning from 150 to 200-kDa in normal muscle. The LGMD2I patient showed a narrower band with a marked lower molecular mass (figure 2). The amount in β-dystroglycan staining was similar to the control muscle. In addition, we observed a reduction of the 300-kDa fragment of laminin-α2 band and a near-absence of the 80-kDa fragment labeling. These findings are in contradiction with the immunohistochemical data, where no special reduction was evident.

Discussion. In this study, we identified two homozygous variations in the *FKRP* gene, 341C>G and 1486T>A, in the affected members of the original Tunisian family suffering from LGMD2I.[3] Together with the linkage studies, our results confirm that *FKRP* gene is responsible for LGMD2I. Testing the alterations in 170 chromosomes from the normal Tunisian population showed no changes for the mutation 1486T>A, whereas the 341C>G variation was found in four chromosomes including a homozygous state. These results suggest that the mutation 1486T>A may be disease causative while the 341C>G variation is likely to be a polymorphism. However, this 341C>G change has previously been described as a mutation in one compound heterozygous MDC1C French patient.[4] The wide range of phenotypes caused by *FKRP* gene mutations[4,5] also suggests that the effect of mutations on FKRP function differ according to mutations. Further functional studies are necessary to elucidate the pathogenic role of each mutation.

Immunohistochemical studies and immunoblot analysis showed that the expression of the α-dystroglycan, but not the β-dystroglycan, was abnormal in muscle of LGMD2I patients. Both α- and β-dystroglycans are coded by a single gene,[6] translated as a single polypeptide precursor and then posttranslationally cleaved to produce the α and β subunits. Synthesis and cleavage of this precursor protein and transport of β-dystroglycan should correctly occur in LGMD2I patients since β-dystroglycan seems to be intact. The monoclonal antibody VIA4-1 is thought to recognize a carbohydrate epitope.[7] Therefore, overall, our results support the idea that posttranslational modification and glycosylation of α-dystroglycan may be altered in patients with *FKRP* gene mutations.[4] Similar findings were reported in patients affected by Fukuyama congenital MD (mutations in *fukutin* gene)[8] and muscle-eye-brain disease (mutations in *POMGnT1* gene),[9] as well as in *myd* mice (mutations in *LARGE* gene).[10] All these proteins, like FKRP are thought to have a role in modifying cell surface molecules, such as glycoprotein and glycolipid.[4,8,9,10]

Immunohistochemical studies showed normal expression of laminin-α2; however, immunoblot analysis

identified a severe reduction of the 300-kDa fragment and a virtual absence of the 80-kDa fragment. Similar findings were reported in other families with mutations in *FKRP* gene.[5] Laminin-α2 is an extracellular matrix protein that binds to the α-dystroglycan in the sarcolemma. This binding plays a key role in the assembly of the extracellular matrix components. We can suggest that hypoglycosylation of the α-dystroglycan due to *FKRP* mutations could alter binding or assembly of the extracellular components causing an abnormal staining of the laminin-α2. The difference between the immunocytochemical and immunoblot analyses could suggest that mutations in *FKRP* gene result in the altered processing, epitope masking, or abnormal folding of the laminin-α2 polypeptide chain.[5]

The identification of *FKRP* as responsible for LGMD2I and MDC1C provided us insights into the molecular mechanism of muscular dystrophy and the roles of glycosylation on α-dystroglycan. However, there remain a number of questions to be solved, including the role of *FKRP* on glycosylation of α-dystroglycan and the variable laminin-α2 expression.

Acknowledgment

The authors thank all sequence team members in the Department of Molecular Biology, Keio University School of Medicine.

References

1. Neuromuscular disorders: gene location. Neuromuscul Disord 2003;13:97–108.
2. De Sandre-Giovannoli A, Chaouch M, Kozlov S, et al. Homozygous Defects in LMNA, Encoding Lamin A/C Nuclear-Envelope Proteins, Cause Autosomal Recessive Axonal Neuropathy in Human (Charcot-Marie-Tooth Disorder Type 2) and Mouse. Am J Hum Genet 2002;70:726–736.
3. Driss A, Amouri R, Ben Hamida C, et al. A new locus for autosomal recessive limb-girdle muscular dystrophy in a large consanguineous Tunisian family maps to chromosome 19q13.3. Neuromuscul Disord 2000;10:240–246.
4. Brockington M, Blake DJ, Prandini P, et al. Mutations in the fukutin-related protein gene (*FKRP*) cause a form of congenital muscular dystrophy with secondary laminin alpha2 deficiency and abnormal glycosylation of alpha-dystroglycan. Am J Hum Genet 2001;69:1198–1209.
5. Brockington M, Yuva Y, Prandini P, et al. Mutations in the fukutin-related protein gene (*FKRP*) identify limb girdle muscular dystrophy 2I as a milder allelic variant of congenital muscular dystrophy MDC1C. Hum Mol Genet 2001;10:2851–2859.
6. Ibraghimov-Beskrovnaya O, Milatovich A, Ozcelik T, et al. Human dystroglycan: skeletal muscle cDNA, genomic structure, origin of tissue specific isoforms and chromosomal localization. Hum Mol Genet 1993;2:1651–1657.
7. Ervasti JM, Campbell KP. Membrane organization of the dystrophin-glycoprotein complex. Cell 1991;66:1121–1131.
8. Hayashi YK, Ogawa M, Tagawa K, et al. Selective deficiency of alpha-dystroglycan in Fukuyama-type congenital muscular dystrophy. Neurology 2001;57:115–121.
9. Kano H, Kobayashi K, Herrmann R, et al. Deficiency of alpha-dystroglycan in muscle-eye-brain disease. Biochem Biophys Res Commun 2002;291:1283–1286.
10. Grewal PK, Holzfeind PJ, Bittner RE, Hewitt JE. Mutant glycosyltransferase and altered glycosylation of alpha-dystroglycan in the myodystrophy mouse. Nat Genet 2001;28:151–154.

Evaluation of essential tremor with multi-voxel magnetic resonance spectroscopy

Fernando L. Pagan, MD; John A. Butman, MD, PhD; James M. Dambrosia, PhD; and Mark Hallett, MD

Abstract—The pathologic substrate of essential tremor (ET) remains unknown. The authors studied 10 patients with ET and 10 volunteers using a multislice MR spectroscopy imaging sequence. Left and right cerebellar hemisphere NAA/CR and NAA/Cho ratios were significantly smaller in the ET patients than healthy subjects. The authors' data suggest that the decreased NAA/Cr and NAA/Cho ratios within the cerebellum may represent an abnormality in neuronal function.

NEUROLOGY 2003;60:1344–1347

MR spectroscopy (MRS) can make in vivo, noninvasive inferences about the neuropathology of CNS disorders. We used a multivoxel, multislice, multimetabolite, MRS-imaging program developed at the National Institutes of Health (NIH)[1,2] to evaluate essential tremor (ET). We measured N-acetylaspartate (NAA), choline (Cho), creatine (Cr), and lactate (Lac). Our main objective was to compare NAA/Cr and NAA/Cho ratios within the cerebellum of ET patients with those from healthy volunteers.

See also page 1232

From the Medical Neurology Branch (Drs. Pagan and Hallett) and Biostatistics Branch (Dr. Dambrosia), National Institutes of Health, National Institute of Neurological Disorders and Stroke; Diagnostic Radiology Department (Dr. Butman), Warren G. Magnuson Clinical Center, Bethesda, MD.

Received May 8, 2002. Accepted in final form February 12, 2003.

Address correspondence and reprint requests to Dr. Mark Hallett, NIH, NINDS, HMCS, Building 10, Room 5N226, 10 Center Drive, MSC1428, Bethesda, MD 20892-1428; e-mail: hallettm@ninds.nih.gov

ELSEVIER

Journal of the Neurological Sciences 211 (2003) 23–28

Journal of the Neurological Sciences

www.elsevier.com/locate/jns

Protein and gene analyses of dysferlinopathy in a large group of Japanese muscular dystrophy patients

Kazuhiko Tagawa[a,b], Megumu Ogawa[a], Kiyokazu Kawabe[a], Gaku Yamanaka[a], Tsuyoshi Matsumura[a], Kanako Goto[a], Ikuya Nonaka[c], Ichizo Nishino[a], Yukiko K. Hayashi[a,*]

[a] *Department of Neuromuscular Research, National Institute of Neuroscience, National Center of Neurology and Psychiatry (NCNP), 4-1-1 Ogawa-higashi, Kodaira, Tokyo 187-8502, Japan*

[b] *Department of Molecular Therapeutics, Tokyo Metropolitan Institute for Neuroscience, 2-6 Musashidai, Fuchu, Tokyo 183-8526, Japan*

[c] *Japan National Center Hospital for Mental, Nervous, and Muscular Dystrophies, NCNP, 4-1-1 Ogawa-higashi, Kodaira, Tokyo 187-8551, Japan*

Received 4 December 2002; received in revised form 30 January 2003; accepted 3 February 2003

Abstract

Mutations in the dysferlin gene cause muscular dystrophies called dysferlinopathy, which include limb-girdle muscular dystrophy type 2B (LGMD2B) and Miyoshi myopathy (MM). To clarify the frequency, clinicopathological and genetic features of dysferlinopathy in Japan, we performed protein and gene analyses of dysferlin. We examined a total of 107 unrelated Japanese patients, including 53 unclassified LGMD, 28 MM and 26 other neuromuscular disorders (ONMD). Expression of dysferlin protein was observed using immunohistochemistry (IHC) and mini-multiplex Western blotting (MMW), and mutation analysis was performed. We found a deficiency of dysferlin protein by both IHC and MMW in 19% of LGMD and 75% of MM patients, and mutations in the dysferlin gene were identified in this group alone. 19% of dysferlin-deficient patients had 3370G → T missense mutation and 16% had 1939C → G nonsense mutation. The patients with homozygous 3370G → T mutation showed milder clinical phenotypes. Twenty-five percent of MM muscles had normal dysferlin protein contents that suggested the genetic heterogeneity of this disease. Altered immunolocalization of dysferlin was observed in not only primary dysferlinopathy, but also in the several diseased muscles with normal protein contents. This result implies the necessity of other protein(s) for proper membrane localization of dysferlin, or some roles of dysferlin in the cytoplasmic region.

Keywords: Limb-girdle muscular dystrophy (LGMD); Miyoshi myopathy (MM); Dysferlin; Immunohistochemistry; Immunoblotting; Mutation analysis; Frequency

1. Introduction

Limb-girdle muscular dystrophy (LGMD) is a group of genetically heterogeneous progressive muscular disorders predominantly involved in proximal limb muscles. The responsible genes and their products were identified in at least 3 autosomal dominant and 10 autosomal recessive forms. Autosomal recessive form of LGMD type 2B (LGMD2B) is caused by mutations of the dysferlin gene (*DYSF*) on chromosome 2p13 [1,2]. Mutations of *DYSF* also cause Miyoshi myopathy (MM), which is predominantly involved in calf muscles, and distal anterior compartment myopathy [1–3]. These diseases caused by mutations in *DYSF* are called as dysferlinopathy. Dysferlin is a FER-1 member protein and contains six putative C2 domains [1,4], which can bind to phospholipids, inositol polyphosphates, Ca^{2+} and intracellular proteins [5,6]. Dysferlin expresses predominantly in skeletal muscle and localizes to the plasma membrane of muscle fibers, and was suggested to be involved in membrane fusion [7,8].

To assess the frequency and clinical and genetic characterization of dysferlinopathy in Japan, we performed protein and gene mutation analyses of dysferlin and other responsible gene products for muscular dystrophy in patients with diseases clinically diagnosed as LGMD and MM.

* Corresponding author. Tel.: +81-42-341-2711; fax: +81-42-346-1742.
E-mail address: hayasi_y@ncnp.go.jp (Y.K. Hayashi).

0022-510X/03/$ - see front matter © 2003 Elsevier Science B.V. All rights reserved.
doi:10.1016/S0022-510X(03)00041-8

2. Materials and methods

2.1. Clinical materials

All clinical materials were obtained for diagnostic purposes with informed consent. The biopsied skeletal muscle specimens were flash-frozen in isopentane chilled with liquid nitrogen. Genomic DNA was isolated either from peripheral blood lymphocytes or biopsied skeletal muscles using a standard technique. We examined a total of 107 unrelated Japanese patients that included 53 unclassified LGMD, 28 MM, and 26 other neuromuscular disorders (ONMD) as diseased controls. ONMD included Duchenne muscular dystrophy (DMD), Becker muscular dystrophy (BMD), inflammatory myopathy, mitochondrial myopathy, congenital myopathy and neuropathy that were diagnosed clinically and histochemically.

2.2. Mini-multiplex Western blotting

This method was the modified multiplex Western blotting described by Anderson and Davison [9]. Ten slices (6 μm thick and approximately 2 mg) of frozen skeletal muscle samples were sonicated in 30-μl aliquots of treatment buffer (125 mM Tris–HCl, 4% SDS, 4 M urea, 5% 2-mercaptoethanol, 10% glycerin, 0.0025% BPB). The samples were treated at 100 °C for 3 min, centrifuged at 10,000 × *g* for 5 min, and 9-μl aliquots of the supernatants were applied to each lane. Mini-PROTEAN3 Electrophoresis System equipment and ready-made 5–10% gradient gels with seven-well (Nippon Bio-Rad Laboratories, Tokyo, Japan) were used. The gels were run at 5 mA overnight in the cold room with stirring and blotted with a limiting current of 1 A for 7 h onto a 0.45-μm PVDF membrane (Nihon Eido, Tokyo, Japan) using Trans-Blot Electrophoretic Transfer Cell with plate electrodes and supercooling coil (Nippon Bio-Rad Laboratories). The equipment was attached to a thermocirculator set at −20 °C. After blotting, the gels were stained using Quick-CBB (Wako, Osaka, Japan). The density of the myosin heavy chain band on the post-blotted gel was estimated, and the amount of skeletal muscle protein was normalized. The cocktail of primary antibodies was prepared with 5% milk in TBST including anti-dystrophin (Dy8/6C5), 1:50; dysferlin (Hamlet), 1:1000; p94/Calpain 3 (Calp3d/2C4), 1:20; α-sarcoglycan (Ad1/20A6), 1:100; β-dystroglycan (43DAG/8D5), 1:1000. The antibodies were available from Novocastra Laboratories, Newcastle-upon-Tyne, UK. After blocking, the membranes were incubated in primary antibodies cocktail for overnight at 4 °C. After the washes, Histofine Simple Stain Max Po (Multi) (Nichirei, Tokyo, Japan) as secondary antibody was diluted 1:5 in TBST and added to the membrane for 1 h at room temperature. The secondary antibody was a peroxidase-conjugated Fab' fragment and was specific to both anti-mouse and anti-rabbit IgG. After the washes, the immunoreactive bands on the membrane were visualized using the POD Immunostain Set (Wako). The immunostained membranes were scanned, and the image data were stored for densitometrical analysis. The amounts of each protein were quantitated as percentages of the control sample by the densitometry technique using Quantity One® (PDI, Huntington Station, NY).

2.3. Immunohistochemistry

Immunohistochemical analysis was performed as previously described [10]. We used antibodies for dysferlin (affinity-purified rabbit polyclonal anti-dysferlin antibody raised against the *SalI* fragment of dysferlin [7], Hamlet and Hamlet-2 (Novocastra Laboratories), α-, β-, γ-, δ-sarcoglycans (Novocastra Laboratories), caveolin-3 (BD Transduction Laboratories, Lexington, KY) and dystrophin (Dy8/6C5 from Novocastra Laboratories).

2.4. Mutation analyses

Polymerase chain reaction single-strand conformational polymorphism (PCR-SSCP) using specific primer sets for each 55 exon of *DYSF* was performed [1]. SSCP analysis of the PCR products was performed using GenePhor DNA Separation System and GeneGel Excel 12.5/24 Kit (Amersham Biosciences., Tokyo, Japan) under each of the three different temperatures of 5, 10 and 15 °C. The PCR products were also directly sequenced using Long Read Tower (Amersham Biosciences), or digested with proper restriction enzymes at the replaced sites.

3. Results

3.1. Immunohistochemistry and mini-multiplex Western blotting

Immunohistochemically, dysferlin is located at the plasma membrane of each skeletal muscle fiber in normal subjects as previously described [7]. However, a total of 107 biopsied limb-muscle specimens we examined in this study showed various immunostaining patterns of dysferlin. We classified the staining patterns into four groups of 'Normal,' a clear membrane staining similar to normal muscles, 'Negative,' the defect of the immunoreaction, 'Faint,' apparently weak immunoreaction at the plasma membrane compared with the normal muscles and 'Abnormal,' cytoplasmic accumulation of immunopositive materials with deficiency of membrane staining or showing positive/negative mosaic membrane staining (Fig. 1).

Fig. 2 showed the results of mini-multiplex Western blotting (MMW). Sample from normal muscle was demonstrated the clear separation and immunostaining of the six bands corresponding to the responsible gene products of muscular dystrophies (lane 1). Dystrophin was displayed at low mobility and was defined the molecular mass of 400

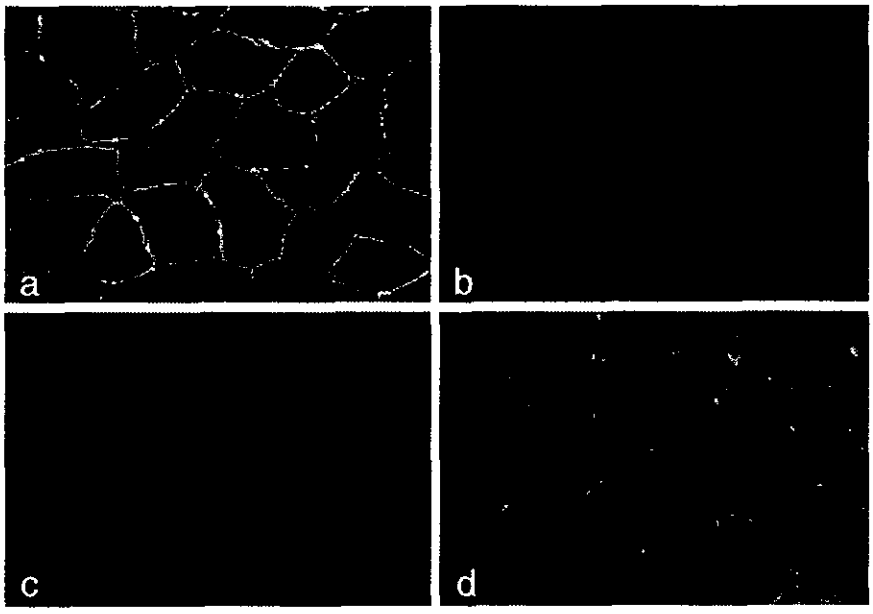

Fig. 1. Immunostaining patterns of dysferlin. Immunostaining patterns were classified to four groups. 'Normal' shows clear membrane staining similar to normal control muscles (a), 'Negative' is defect of the immunoreaction (b), 'Faint' reveals apparently weak immunoreaction at the plasma membrane compared to the control muscles (c), and 'Abnormal' shows cytoplasmic accumulation of immunopositive materials or positive/negative mosaic staining patterns (d).

kDa. The bands of dysferlin, α-sarcoglycan and β-dystroglycan were represented at 230, 50 and 43 kDa, respectively. p94/calpain 3 was found as two bands at 94 and 30 kDa. The former was the full length of the gene product, and the latter was the N-terminal fragment [11]. p94/calpain 3 bands were not seen in lane 2, although the amount of dystrophin, dysferlin, α-sarcoglycan and β-dystroglycan proteins were normal values on MMW. The mutation of p94/calpain 3 gene in this patient was previously identified and diagnosed as LGMD2A [12]. Lane 3 showed a deficiency of dysferlin band, although the other four proteins were normal. We identified a homozygous mutation (3370G→T) of *DYSF* in this patient and diagnosed as LGMD2B. A DMD patient showed a defect of the dystrophin band and reduced amounts of α-sarcoglycan and β-dystroglycan (lane 4).

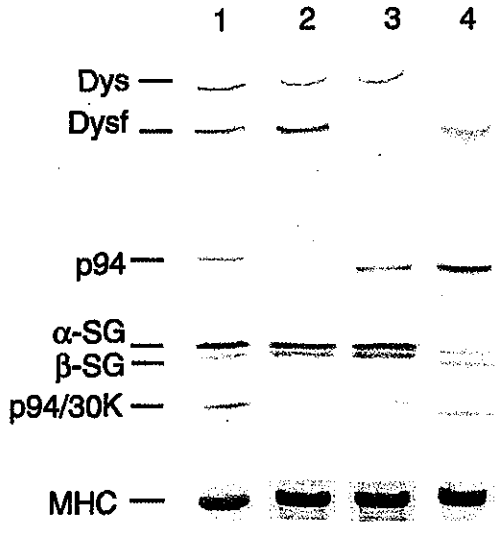

Fig. 2. Mini-multiplex Western blotting (MMW). Samples from normal control subjects demonstrated the six bands corresponding to dystrophin, dysferlin, p94/calpain 3, α-sarcoglycan, β-dystroglycan and N-terminal fragment of p94/calpain 3 (30K) (lane 1). LGMD2A shows deficiency of p94/calpain 3 and p94/30K bands, although the other four proteins were normal (lane 2). LGMD2B shows markedly reduced amounts of dysferlin protein; however, the amount of other proteins are normal (lane 3). DMD showed a defect of the dystrophin band and reduced amounts of α-sarcoglycan and β-dystroglycan (lane 4). MHC: myosin heavy chain.

From the result of densitometrical analysis, the amounts of dysferlin protein showed a biphasic pattern of less than 21% and greater than 37% of the control sample, and we defined less than 30% as 'Deficient'.

3.2. Protein analyses of LGMD patients

Among 53 skeletal muscles from unrelated LGMD patients, 10 (19%) showed 'Deficient' of dysferlin protein on MMW. Nine of these ten muscles showed 'Negative,' and one showed 'Faint' immunoreaction of dysferlin staining.

A total of 43 of 53 (81%) of LGMD muscles showed more than 30% of dysferlin protein contents by MMW. However, only 16 patients showed 'Normal' immunostaining pattern and 27 showed altered staining patterns of dysferlin. Interestingly, two cases showed 'Negative' membrane staining, although the protein contents were normal. By protein and gene analyses, we identified 11 LGMD2A and one LGMD1C patients in this group [13]. Two muscles

Table 1
Mutations identified in the dysferlin-deficient patients

Patient number	Mutation		Clinical diagnosis	IHC/MMW
1	3370G→T	Homozygous	LGMD	negative/decreased
2	3370G→T	Homozygous	LGMD	negative/decreased
3	3370G→T	Homozygous	LGMD	negative/decreased
4	3370G→T	Homozygous	MM	abnormal/decreased
5	3370G→T/?	Heterozygous	LGMD	negative/decreased
6	3370G→T/ 1939C→G	Heterozygous	LGMD	faint/decreased
7	1939C→G/ 5882G→T	Heterozygous	MM	faint/decreased
8	1939C→G/?	Heterozygous	MM	negative/decreased
9	1939C→G/?	Heterozygous	MM	negative/decreased
10	1939C→G/?	Heterozygous	MM	faint/decreased
11	3746Gdel/ 3017-2A→G*	Heterozygous	MM	negative/decreased
12	3746Gdel	Homozygous	MM	negative/decreased
13	1657+2T→C*	Homozygous	MM	negative/decreased
14	2090G→T	Homozygous	MM	negative/decreased
15	3016+1G→A*	Homozygous	LGMD	negative/decreased

*Novel mutations.

from LGMD2A patients showed 'Normal' immunolocalization of dysferlin, while nine LGMD2A and one LGMD1C showed either 'Faint' or 'Abnormal' staining patterns with normal dysferlin protein contents.

3.3. Protein analyses of MM patients

A total of 21 of 28 (75%) MM patients showed 'Deficient' of dysferlin protein less than 30% of control value on MMW, and all these patients showed altered immunostaining patterns, including 14 'Negative', 5 'Faint' and 2 'Abnormal'. On the other hand, seven patients who were clinically diagnosed as MM showed normal dysferlin protein contents by MMW with variable immunostaining patterns, including one 'Negative.'

3.4. Protein analysis of OMND

All ONMD patients showed normal protein contents by MMW; however, only 13:26 (50%) showed 'Normal' immunostaining pattern of dysferlin. The remaining 13 biopsied samples including BMD, inflammatory myopathy, congenital myopathy and neuropathy showed either 'Faint' or 'Abnormal' immunostaining patterns of dysferlin. There was no specimen with 'Negative' dysferlin staining.

3.5. Mutation analyses of DYSF

The 31 (10 LGMD and 21 MM) patients who showed 'Deficient' of dysferlin protein with altered immunostaining patterns were suggested to be primary dysferlinopathy, and mutation analyses of *DYSF* were performed. We examined all 55 exons of *DYSF* in 14 patients. With the remaining 17 patients, we could only examine three exons of 18, 28 and 31 because of the limited amounts of the samples. We found 8 kinds of mutations in 15 patients including 3 novel splice-site mutations (Table 1). Mutation analyses revealed that the 3370G→T (W999C) missense mutation in exon 28 was most frequently observed, and 19% (6:31) of dysferlin-deficient patients had this mutation. Five patients (three were homozygous, two were compound heterozygous) were LGMD, and one homozygous patient was MM. From the clinical point of view, all four patients with the homozygous 3370G→T mutation showed milder phenotypes. The age of onset was later than the third decade of life (Fig. 3), and only one patient used a wheelchair after 60 years old. The 1939C→G (Y522X) mutation in exon 18 was also frequently observed, and 16% (5:31) dysferlin-deficient patients including four MM and one LGMD showed this mutation heterozygously (Table 1). This LGMD patient was a compound heterozygote with frequently observed 3370G→T and 1939C→G mutations (patient 6 in Table 1). Interestingly, a sister of this patient with identical mutations had a diagnosis of MM. Two patients had the 3746G deletion in exon 31, and this frame-shift mutation was observed only in MM patients. No mutations in the *DYSF* were found in seven MM patients with normal protein contents. None in 100 control Japanese individuals had these mutations by enzyme digestion of the genomic PCR products using *Ava*II (for 3370G→T) and *Sau*3AI (for 1939C→G), or PCR-SSCP analysis.

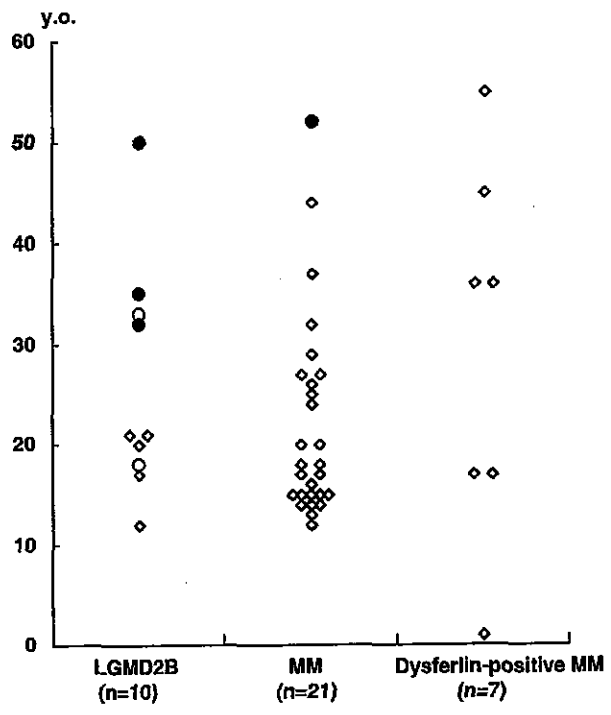

Fig. 3. The age of onset of the patients with LGMD2B, MM and MM with normal dysferlin protein. Patients with the 3370G→T mutation are described as ● (homozygous) and ○ (heterozygous).

3.6. Histopathological analysis of biopsied muscles

All biopsied muscle specimens from primary dysferlinopathy patients showed dystrophic changes in the variation of fiber diameters with necrotic and regenerating fibers. Type 1 fiber predominance was observed in 31% of the samples, 19% contained lobulated fibers and 12% had some rimmed vacuoles. Inflammatory changes are common features in the dysferlinopathy [8,14–16], and we observed that 11% of patients showed mild inflammatory changes with perivascular cellular infiltration. One MM patient showed markedly different pathological findings between gastrocnemius and biceps muscles taken at the same time (data not shown). The gastrocnemius muscle showed advanced dystrophic changes with marked infiltration of fatty and connective tissues, although a specimen from the biceps muscle showed only minimal myopathic changes.

4. Discussion

From the dysferlin protein analysis by both immunohistochemistry (IHC) and MMW, we found 31 among 107 unrelated patients showed abnormal immunostaining patterns of dysferlin with less than 30% of protein contents. These patients were suggested to be primary dysferlinopathy, and in fact, mutations of *DYSF* could be identified in this group alone. Among 53 unclassified LGMD, 10 patients were in this group and suspected to be LGMD2B. That is, the frequency of LGMD2B was 19% in the present study. LGMD2A was estimated at 21% (11:53) of LGMD patients from the protein analysis in this study and 26% in the previous study [12]. From these results, LGMD2B will be the second frequent type of LGMD in Japan.

We found 8 kinds of mutations among 15 dysferlin-deficient patients, including 3 novel splice-site mutations. The 3370G → T mutation (W999C) in exon 28 was most frequently observed in the present study and 19% (6:31) of putative primary dysferlinopathy patients showed this mutation. The result that a half (5:10) of dysferlin-deficient LGMD patients had the 3370G → T mutation will be helpful for mutation screening of Japanese LGMD2B patients. Only one patient with MM had the same 3370G → T mutation homozygously, who showed very mild distal muscle weakness. The patients with the homozygous 3370G → T missense mutation showed later onset of the disease and milder muscle weakness among the patients with dysferlinopathy. Dysferlin protein with W999C substitution caused by the 3370G → T mutation may have some limited roles even though the protein was barely detectable by MMW in all homozygous patients.

The 1939C → G mutation (Y522X) in exon 18 was also frequently observed and 16% (5:31) of dysferlin-deficient patients showed this mutation heterozygously. Four patients with this mutation were MM, and the frequency of the 1939C → G mutation in MM was 19% (4:21). Only one patient with 1939C → G showed LGMD type who had the compound heterozygous mutation of 3370G → T, and his sister with the same mutations showed MM-type phenotype. The mutation of the 3746G deletion was identified only in patients with MM. Further investigations may be helpful to clarify the genotype–phenotype correlation of the disease.

It is unclear why some patients showed LGMD-type and others showed MM-type muscle involvement, even though they had the same mutation. In the present study, we found identical mutations in a family that had different clinical phenotypes. There are also some reports that described the different distributions of affected muscles between patients with the same mutation from one family [17–19]. It is also unclear why the severity of muscle involvement was so different between muscles even in the same patient. Additional unknown factors may exist which determine or modify clinical phenotypes of dysferlinopathy.

It should be noted that only 75% of MM patients showed deficiency of the dysferlin protein. The remaining 25% of patients with diseases diagnosed as MM clinically had normal dysferlin protein contents with no mutation in the dysferlin gene. Clinical severity and the age at onset of these patients were variable; however, serum CK levels were lower than dysferlinopathy (data not shown). Some families of MM phenotype were also reported to have no linkage to chromosome 2 [20]. These results conform the genetic heterogeneity of MM phenotype.

Altered immunostaining patterns of dysferlin with normal protein content were observed in various diseased muscles including BMD and LGMD other than type 2B in the present study. Interestingly, these changes were not specific to the disease, because for example, some LGMD2A patients showed 'Faint' or 'Abnormal' immunostaining patterns by IHC, but other LGMD2A showed 'Normal' staining pattern of dysferlin. Furthermore, three of diseased muscles showed negative membrane staining of dysferlin with normal protein contents. We previously reported that caveolin-3 and dysferlin are co-immunoprecipitated, and LGMD1C patients with a mutation in the caveolin-3 gene showed an abnormal immunostaining pattern of dysferlin [13]. This result may imply the abnormality of dysferlin-associated molecule(s) in the plasma membrane of skeletal muscle causes instability in the membrane localization of dysferlin. Either dysferlin may have some roles not only on the plasma membrane but also in the cytoplasmic region. The function of dysferlin is not known; however, dysferlin was suggested to be involved in membrane fusion [7]. Abnormal localization of dysferlin may reflect a very early stage of structural alteration or functional damage of muscle membrane in several disorders, or abnormalities in the dysferlin-related protein(s) on the plasma membrane. To clarify the role of dysferlin and its associated protein(s) may be helpful to understand the localization and functions of dysferlin.

Acknowledgements

We dedicate this article to the memory of Dr. Kiichi Arahata (National Institute of Neuroscience, NCNP), who passed away while this project was underway. We thank Drs. L.V.B. Anderson and K.M.D. Bushby (Newcastle-upon-Tyne, UK) for their helpful advice on multiplex Western blotting analysis. This work was supported by Grants-in-Aid for Scientific Research for Center of Excellence (COE) and Research on Psychiatric and Neurological Diseases and Mental Health from the Ministry of Health, Labour and Welfare, and Ichiro Kanehara Memorial Foundation, Japan.

References

[1] Liu J, Aoki M, Illa I, et al. Dysferlin, a novel skeletal muscle gene, is mutated in Miyoshi myopathy and limb girdle muscular dystrophy. Nat Genet 1998;20:31–6.
[2] Bashir R, Britton S, Strachan T, et al. A gene related to *Caenorhabditis elegans* spermatogenesis factor fer-1 is mutated in limb-girdle muscular dystrophy type 2B. Nat Genet 1998;20:37–42.
[3] Illa I, Serrano-Munuera C, Gallardo E, et al. Distal anterior compartment myopathy: a dysferlin mutation causing a new muscular dystrophy phenotype. Ann Neurol 2001;49:130–4.
[4] Britton S, Freeman T, Vafiadaki E, et al. The third human FER-1-like protein is highly similar to dysferlin. Genomics 2000;68:313–21.
[5] Nalefski EA, Falke JJ. The C2 domain calcium-binding motif: structural and functional diversity. Protein Sci 1996;5:2375–90.
[6] Rizo J, Sudhof TC. C2-domains, structure and function of a universal Ca^{2+}-binding domain. J Biol Chem 1998;273:15879–82.
[7] Matsuda C, Aoki M, Hayashi YK, Ho MF, Arahata K, Brown Jr RH. Dysferlin is a surface membrane-associated protein that is absent in Miyoshi myopathy. Neurology 1999;53:1119–22.
[8] Anderson LV, Davison K, Moss JA, et al. Dysferlin is a plasma membrane protein and is expressed early in human development. Hum Mol Genet 1999;8:855–61.
[9] Anderson LV, Davison K. Multiplex Western blotting system for the analysis of muscular dystrophy proteins. Am J Pathol 1999;154:1017–22.
[10] Hayashi YK, Ogawa M, Tagawa K, et al. Selective deficiency of α-dystroglycan in Fukuyama-type congenital muscular dystrophy. Neurology 2001;57:115–21.
[11] Anderson LV, Davison K, Moss JA, et al. Characterization of monoclonal antibodies to calpain 3 and protein expression in muscle from patients with limb-girdle muscular dystrophy type 2A. Am J Pathol 1998;153:1169–79.
[12] Chae J, Minami N, Jin Y, et al. Calpain 3 gene mutations: genetic and clinico-pathologic findings in limb-girdle muscular dystrophy. Neuromuscular Disord 2001;11:547–55.
[13] Matsuda C, Hayashi YK, Ogawa M, et al. The sarcolemmal proteins dysferlin and caveolin-3 interact in skeletal muscle. Hum Mol Genet 2001;10:1761–6.
[14] Rowin J, Meriggioli MN, Cochran EJ, Sanders DB. Prominent inflammatory changes on muscle biopsy in patients with Miyoshi myopathy. Neuromuscular Disord 1999;9:417–20.
[15] McNally EM, Ly CT, Rosenmann H, et al. Splicing mutation in dysferlin produces limb-girdle muscular dystrophy with inflammation. Am J Med Genet 2000;91:305–12.
[16] Gallardo E, Rojas-Garcia R, de Luna N, Pou A, Brown Jr RH, Illa I. Inflammation in dysferlin myopathy: immunohistochemical characterization of 13 patients. Neurology 2001;57:2136–8.
[17] Weiler T, Bashir R, Anderson LV, et al. Identical mutation in patients with limb girdle muscular dystrophy type 2B or Miyoshi myopathy suggests a role for modifier gene(s). Hum Mol Genet 1999;8:871–7.
[18] Illarioshkin SN, Ivanova-Smolenskaya IA, Greenberg CR, et al. Identical dysferlin mutation in limb-girdle muscular dystrophy type 2B and distal myopathy. Neurology 2000;55:1931–3.
[19] Nakagawa M, Matsuzaki T, Suehara M, et al. Phenotypic variation in a large Japanese family with Miyoshi myopathy with nonsense mutation in exon 19 of dysferlin gene. J Neurol Sci 2001;184:15–9.
[20] Linssen WH, de Visser M, Notermans NC, et al. Genetic heterogeneity in Miyoshi-type distal muscular dystrophy. Neuromuscular Disord 1998;8:317–20.